



UNIVERSITÀ DEGLI STUDI DI PADOVA
Department of Comparative Biomedicine and Food Science-
BCA

Second Cycle Degree (MSc)
In Biotechnologies for Food Sciences

“Metabolomics by ^1H -NMR and mineral content by ICP-OES for the spectroscopic characterization of the rumen of dairy cows: an in vitro fermentation experiment”

Supervisor:

Prof. Fabio Vianello

Co-supervisor:

Prof. Lucio Zennaro

Dr. Anna Damato

Submitted by:

Esmail Montazeri Najafabadi

Student N. 2012964

ACADEMIC YEAR 2022-2023

Table of Contents

| Title | Page |
|----------------------------------------------------------------------|------|
| 1. Summary..... | 1 |
| 2. Introduction..... | 2 |
| 2.1. Rumen fermentations and composition of rumen fluid..... | 2 |
| 2.2. Ruminal fluid metabolomics..... | 4 |
| 2.3. NMR spectroscopy..... | 4 |
| 2.3.1 Pros and cons..... | 4 |
| 2.3.2. Theoretical principles..... | 5 |
| 2.3.3. Metabolic Profile Analysis (Metabolomics)..... | 9 |
| 2.3.4. Statistical analysis of spectroscopic data (Metabonomic)..... | 9 |
| 2.3.5. PCA and classification..... | 10 |
| 2.3.5.1. PLS, PLS-DA..... | 12 |
| 2.3.5.2. Selecting proper input variables..... | 13 |
| 2.3.6. Generating bucket tables..... | 13 |
| 2.3.7. Rectangular bucketing (1D/2D NMR, LC-MS)..... | 14 |
| 2.3.7.1. Point-wise bucketing (1D NMR)..... | 14 |
| 2.3.7.2. Variable size bucketing (1D NMR)..... | 14 |
| 2.3.7.3. Advanced bucketing (1D NMR, LC-MS)..... | 15 |
| 2.3.7.4. Bucket table calculation with 1D NMR spectra..... | 15 |
| 2.3.8. Generating other tables (Y table)..... | 17 |
| 2.3.9. PCA..... | 18 |
| 2.3.9.1. Basic PCA..... | 18 |
| 2.3.9.2. Some remarks..... | 19 |
| 2.4. ¹ H-NMR: metabonomic analysis..... | 24 |
| 2.5. ICP-OES Applications..... | 25 |
| 2.5.1. Agricultural and Foods..... | 26 |
| 2.5.2. Biological and Clinical..... | 26 |
| 2.6. GENERAL CHARACTERISTICS OF ICP-OES..... | 26 |
| 2.6.1. Detection of Emission..... | 26 |
| 2.6.2. Extraction of Information..... | 27 |
| 2.6.3. Performance Characteristics..... | 28 |
| 2.7. Comparing ICP-OES against other methods..... | 28 |
| 2.8. Clay Minerals..... | 29 |
| 2.8.1. Properties..... | 29 |
| 2.8.2. Mineral Structure of Clays..... | 30 |

| | |
|------------------------------------------------------------------------------------|----|
| 2.8.3. Bentonite..... | 31 |
| 2.8.4. Bentonite as a food additive for livestock | 32 |
| 3. Materials and Methods | 32 |
| 3.1. Animal recruitment and care | 32 |
| 3.2. Sample preparation for in vitro fermentation | 33 |
| 3.2.1. In vitro procedure to study fermentation kinetics with ANKOM RF | 34 |
| 3.3. ¹ H-NMR spectroscopy of rumen fluid..... | 40 |
| 3.3.1. Preparation of rumen fluid samples | 40 |
| 3.3.2. Acquisition of NMR spectra..... | 41 |
| 3.3.3. Qualitative analysis of ¹ H-NMR spectra | 42 |
| 3.3.4 Evaluation of mineral and heavy metals content..... | 43 |
| 3.4. Data analysis and statistical processing..... | 43 |
| 3.4.1. Multivariate Statistical Analysis: Principal Component Analysis (PCA) | 43 |
| 4. Result and discussion..... | 46 |
| 4.1 Results of metabolomic analysis by ¹ H-NMR..... | 46 |
| 4.2. Results of the mineral and heavy metal content by ICP-OES | 48 |
| 5. Conclusion | 49 |
| 6. Acknowledgment..... | 49 |
| 7. Reference | 51 |

List of tables

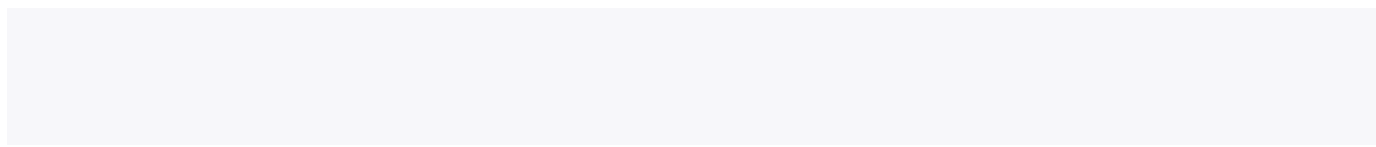
| Title | Page |
|------------------------------------------------------------------------------------------------------------------------------------------------------------------------------------------------------------------------------------|------|
| Table 1.1. Composition of the diet administered to the 6 cows during the entire experimental period. | 33 |
| Table 1.2. Feeding composition for dairy cows | 35 |
| Table 1.3. Regression analysis between the dose of bentonite and mineral concentrations. Only minerals that showed a significant Standardized Regression Coefficient (Beta) with increasing dosage of bentonite are reported. | 49 |

List of figures

| Title | Page |
|-----------------------------------------------------------------------------------------------------------------------------------------------------------------------------------------------------------------------------------------------------------------------------------------------------------------------------------------------------------------------------------------------------------------------------|------|
| Figure 1.1. Orientations that the magnetic moment of an atomic nucleus with non-zero spin can assume when immersed in a magnetic field B_0 | 6 |
| Figure 1.2. Rotation of the Macroscopic Magnetization vector M_0 in the XY plane around the z axis..... | 8 |
| Figure 1.3. Transformation of the FID generated by a single type of nucleus into the corresponding signal in the NMR spectrum..... | 8 |
| Figure 1.4. Transformation of the FID of a complex molecule into the corresponding signal in the NMR spectrum..... | 9 |
| Figure 1.5. Example of an NMR spectrum..... | 9 |
| Figure 1.7. Schematic display of available bucketing techniques | 14 |
| Figure 1.8. Available bucketing techniques for 1D NMR spectra | 15 |
| Figure 1.9. Bucket parameters as used for rectangular bucketing in NMR..... | 16 |
| Figure 1.10. Generating a new Y table..... | 17 |
| Figure 1.11. Commands related to PCA..... | 18 |
| Figure 1.12. Scaling of columns prior to PCA calculations | 18 |
| Figure 1.13. Selecting the dimension of the model space. | 19 |
| Figure 1.14. Typical display after a PCA calculation..... | 20 |
| Figure 1.15. Definition of the PCA display..... | 20 |
| Figure 1.16. Loadings Plot 1D (panel A) and 2D (panel B)..... | 22 |
| Figure 1.17. Interpretation of 2D scores/loadings plots | 23 |
| Figure 1.18. Hotellings_Plot_T2_with_Confidence_Intervals_Ellipses | 23 |
| Figure 1.19. 3D scores plot with Hotellings T2 ellipse. | 24 |
| Figure 1.20. Calibration curve used for ICP-OES..... | 27 |
| Figure 1.21. The 1:1 layer phyllosilicate structure..... | 31 |
| Figure 1.22. The 2:1 layer phyllosilicate structure..... | 31 |
| Figure 1.23. The 2:1:1 layer phyllosilicate structure..... | 31 |
| Figure 1.24. Identification of the spectral signals relating to the metabolites studied on the ^1H -NMR spectrum of one of the rumen liquid samples (blue) and comparison with the spectra obtained from the single standards. Numeric code: 1: Acetate; 2: Propionate; 3: Butyrate; 4: Lactate. Color code: Blue: rumen fluid; Red: Na-Lactate; Green: Na-Butyrate; Purple: Na-Propionate; Black: Na-Acetate..... | 42 |
| Figure 1.25. Example of scores plot (top) and loadings plot (bottom). In particular, the scores of cluster A are spectra similar to each other but different from the spectra of cluster B..... | 45 |
| Figure 1.26. Typical ^1H -NMR spectrum obtained from Rumen Fluid samples. 1. Butyrate, 2. Valine, 3. Propionate, 4. Leucine, 5. Isoleucine, 6. Ethanol, 7. Alanine, 8. Acetate, 8a. Acetate satellite, 9. Isovalerate, 10. Acetylcarnitine, 11. Succinate, 12. Dimethylamine, 13. Methylamine, 14. Sarcosine, 15. | |

Trimethylamine, 16. Oxoglutarate, 17. Carnitine, 18. Glucose, 19. Galactose, 20. Tyrosine, 21. Histidine, 22. Phenylalanine, 23. Tryptophane, 24. Formate47

Figure 1.27. Scores plot (left) and loadings plot (right) of the two first principal components (PC1 and PC2) of the PCA analysis: Each point in the Scores plot represents a sample, in the loadings plot represents a spectral region.....48



1. Summary

The aim of this thesis is to investigate the suitability of two techniques, Proton Nuclear Magnetic Resonance (^1H NMR) and Inductively Coupled Plasma- Optical Emission Spectroscopy (ICP-OES), for the preliminary study of the effects of the administration of zootechnical bentonite, a mineral aflatoxins adsorbent, on the rumen of dairy cows.

Clay minerals, such as bentonite, are added to animal diets because of their capability to absorb heavy metals and mycotoxins, and this practice has been connected to a wide variety of beneficial impacts, particularly on animal health and production. On the other hand, it appears that these materials could also cause adverse effects and interact with the microbiota in the intestinal and ruminal tracts. The current study aims to evaluate the effects of varying doses of bentonite on ruminal fermentations, metabolomes, and mineral content during an *in vitro* fermentation experiment in order to draw conclusions about how these factors are affected. An esophageal probe was used to extract ruminal fluid from a healthy Holstein dairy cow for *in vitro* fermentation. The cow received a total mixed ratio (TMR) diet that included corn and grass silages, cereals, soybean meal, and a vitamin-mineral premix. 50 mL of filtered ruminal fluid, 100 mL of Menke medium, and 1 g of dried TMR utilized *in vivo* were combined to make fermentation bottles. Five treatment groups (B0, B50, B100, B200, and B1000) in a total volume of 150 mL of the previous mixture were used in the study, each with a different bentonite dosage (0, 2.5, 5, 10, and 50 mg). For 24 hours, five samples from each treatment group were incubated at 39 °C. To learn more about the effects of bentonite treatment on ruminal fluid, the metabolome and mineral content of the treated ruminal fluids were evaluated using proton (^1H) nuclear magnetic resonance (NMR) spectroscopy and inductively coupled plasma optical emission spectroscopy (ICP-OES), respectively, in pooled replicate samples. The rumen fluid samples after the *in vitro* fermentation were frozen at -80 °C and analyzed using ^1H -NMR spectroscopy and ICP-OES.

The ^1H -NMR study led to the identification of twenty distinct metabolites and revealed that the treatments resulted in clearly different rumen metabolic profiles for each bentonite dosage. According to the results of the ICP-OES analysis, the addition of bentonite changed the concentration of several elements, including Al, Ba, Ca, Cr, Mn, Mo, and Sr. It is possible that the administration of bentonite does not influence the gross fermentations that take place in the rumen, but it does appear to modify the ruminal metabolome, particularly the concentration of butyrate and propionate, and the concentrations of a few minerals in the ruminal fluid.

Key words: Bentonite, ^1H NMR, Metabolomics, Rumen Fermentation, *In Vitro*

2. Introduction

2.1. Rumen fermentations and composition of rumen fluid

The rumen, together with the reticulum and the omasum, form the important pre-stomach apparatus of ruminants that separates the esophagus from the glandular stomach, or the abomasum, and which acts as a real fermentation chamber for food. In adult cattle, the abomasum has a capacity of between 142 and 148 liters and, together with the reticulum, constitutes more than 80% of the volume of forestomachs. Its stratified squamous epithelium does not produce digestive enzymes, unlike the abomasal mucosa, but rises in papillae responsible for the absorption of the products of fermentation that occur in the lumen of the bowel (Dellmann and Eurell, 2000; Nickel et al., 1979). It is believed that 1 milliliter of rumen fluid contains 10–50 billion bacteria, 1 million protozoa, and thousands of fungi and yeasts, which together make up the symbiotic microflora that facilitates this fermentation process (Saleem et al., 2013). These ruminal microorganisms coexist in constant competition for the metabolism of the organic matter from which the final products are derived, which are then absorbed by the ruminant and essential for its survival and production. The anaerobic environment that makes fermentation possible is guaranteed by a small number of anaerobic bacteria that use small amounts of oxygen from the blood or from the outside through ingestion.

Therefore, in terms of numbers, bacteria make up the majority of the rumen's microbial community. They are classified conventionally on the basis of the substrates they use or the end products of their metabolism.

Among the primary bacteria responsible for the digestion of carbohydrates are amylolytic and cellulolytic bacteria, which produce digestive enzymes that break down the α -glycosidic bonds of starch and soluble carbohydrates and the β -glycosidic bonds of cellulose. The breakdown of these polysaccharides releases the glucose required for bacterial glycolysis, which creates pyruvate, which is then transformed into volatile fatty acids (VFA), the primary energy source for the ruminant, by the anaerobic flora. The three main VFAs are acetic acid, propionic acid, and butyric acid. According to the concentration gradient, 70–80% of these are absorbed at the rumen and reticulum levels by passive transepithelial transport. More specifically, the absorption of VFAs happens through simple diffusion for molecules in their undissociated form and through facilitated diffusion in opposition to bicarbonate ions HCO_3^- for molecules that are dissociated anions (acetate, propionate, butyrate) or those that are present in higher concentrations. Since acetate has a low relative absorption rate, too much of it might cause the rumen's pH to drop by accumulating there. Propionate is transported to the liver after being absorbed by the rumen-reticular mucosa, where it is almost entirely transformed into glucose. In contrast, acetic acid almost entirely escapes the hepatic metabolism by entering the peripheral circulation, where it is used as an energy substrate and a precursor to milk lipids. The ruminal epithelium converts butyrate almost totally into the ketone hydroxybutyrate, which is then circulated and used as an energy source by the

heart, skeletal, and cardiac muscles, as well as by adipose tissue and the central nervous system (Sjaastad et al., 2010).

Lactic acid is another product of the bacterial breakdown of polysaccharides. It is produced in modest amounts in the presence of a balanced diet, the majority of which is quickly converted into propionic acid by the rumen bacteria, and only a small amount is absorbed by the rumen mucosa (Sjaastad et al., 2010). According to Braun et al. (1992), an excess of these result in a buildup of lactic acid in the rumen and a much lower pre-muscle pH, which causes the condition known as rumen acidosis. Its production rises in direct proportion to the rise in highly fermentable carbohydrates.

Proteolytic bacteria can break down dietary proteins into peptides and amino acids that are then used to create microbial proteins either directly or, for the most part, following deamination in ammonia and VFA. Once the various pre-stomachal microorganisms are lysed and digested in the abomasum and the small intestine, microbial proteins provide a source of amino acids for the ruminant (Sjaastad et al., 2010). Finally, secondary bacteria include methane bacteria, which reduce CO₂ with H₂ by releasing methane (CH₄) (Danielsson et al., 2017).

Moving on to rumen protozoa, these are primarily obligate anaerobes that may digest all bacterial material as well as plant matter. VFAs, lactate, and gases like carbon dioxide and hydrogen are also produced by them. They can also accumulate glucose in the form of glycogen in the cytoplasm; in this way, they modulate bacterial glycolysis, limiting the risk of acidosis when the starch content becomes high. Lou et al. (2007) showed that by expanding the surface that cellulolytic bacteria are exposed to, fungi contribute to the destruction of plant fibers that contain lignin, which is primarily found in straw (Akin and Borneman, 1990).

Lipids, which are present in forages in the form of free long-chain fatty acids (mostly palmitic, linoleic, and oleic acids), galactolipids, or triglycerides, are also impacted by bacterial and protozoal fermentation. Galactose and glycerol from the latter two are quickly hydrolyzed in the rumen, where they are converted to VFA. Polyunsaturated fatty acids, on the other hand, are reduced to monounsaturated or saturated fatty acids (Harfoot, 1981). In the dissolved rumen content, there is no lack of minerals taken from the diet: inorganic cations (Na⁺, K⁺, Mg²⁺, Ca²⁺, NH₄⁺, and others) and inorganic anions (Cl⁻, HCO₃⁻, HPO₄²⁻, H₂PO₄⁻, and others). Rumen absorption of cations is reduced compared to that of anions due to the negative electric potential of the ruminal epithelium for the blood (Hoover and Miller, 1991; Sjaastad et al., 2010).

In conclusion, rumen fluid is composed of water, intake, rumen microorganisms, minerals, products of metabolism, and fermentation gas. This complicated heterogeneous combination has a temperature between 38 °C and 41 °C, an osmolarity of around 300 mOsm compared to the forage, which increases to 400 mOsm following food intake, and a pH between 5.8 and 7 (Garrett et al., 1999). (Hoover and Miller, 1991).

2.2. Ruminal fluid metabolomics

Rumen fluid is, therefore, a heterogeneous and complex fluid whose chemical composition reflects the interactions between microflora and diet both in a physiological and pathological sense, becoming an index of the state of health and well-being and of the quantity and quality of the ruminant's productions (Saleem et al., 2012). Metabolomics is the study and measurement of all metabolites that are present in a biological sample (Zhang et al., 2012). Metabonomics, on the other hand, deals with finding and quantifying differences or variations in metabolic profiles between the samples constituting the set of samples under examination in relation to stimuli like nutrition, drugs, and diseases (Nicholson and Lindon, 2008). Recently, a team of researchers, Saleem et al. (2012), used a variety of techniques to characterize the entire metabolome of bovine ruminal fluid and created a database called the Bovine Rumen Database (BRDB) available online (<http://www.rumendb.ca>) that has become the reference for those involved in rumen metabolism. At present it contains information on 335 rumen metabolites with their defined chemical structures. The research revealed that inorganic anions, gases, amino acids, phospholipids, short-chain fatty acids, diglycerides, triglycerides, dicarboxylic acids, VFA, carbohydrates, and esters of the cholesterol make up the majority of the rumen fluid's composition, in agreement with previous authors. Acetate, propionate, butyrate, valerate, glucose, isobutyrate, isovalerate, glutamate, methylamine, formate, phenylacetate, tricarboxylic acids, and hypoxanthine are among the most prevalent organic metabolites identified.

Saleem et al. (2012) combined numerous approaches to identify the different metabolites, including gas chromatography-mass spectrometry, inductively coupled plasma mass spectrometry, mass with direct flow injection (DFI-MS/MS), lipidomic analysis by converting fatty acid methyl esters and gas chromatography-mass spectrometry, as well as the Limulus amoebocyte lysate test (LAL) for endotoxin research. What clearly emerges from their findings is that a simple method is unable to adequately cover the panel of compounds found in rumen fluid. However, one of the most effective and widely applied methods is Nuclear Magnetic Resonance (NMR) spectroscopy (Goldansaz et al., 2017).

2.3. NMR spectroscopy

As previously mentioned, one of the most commonly used analytical methods in both metabolomics and metabonomics is nuclear magnetic resonance (NMR) spectroscopy. Nuclear magnetic resonance is a very potent instrumental analytical technique that enables the collection of precise data through the quantifiable phenomena of energy absorption and subsequent release by atomic nuclei energized by radiofrequency radiation and subjected to a static magnetic field.

2.3.1 Pros and cons

It has many benefits, including the use of reliable technology, simple and minimal sample preparation requirements, and a direct correlation between the concentration of each molecule and the area occupied

by the corresponding NMR signal. When performed on the proton nuclei (^1H), ^1H -NMR allows the detection of all molecules containing hydrogen (including most organic and some inorganic molecules). The sample that is being analyzed has not been modified and is still available for additional NMR experiments or other potential analyses. Although there are benefits, there are also drawbacks, including high cost of the instrumentation, a lack of sensitivity (limited to micromolar and millimolar ranges), and a lack of ability to detect non-protonated compounds and inorganic ions (Goldansaz et al., 2017; Sundekilde et al., 2013).

Despite this, Nuclear Magnetic Resonance spectroscopy is still regarded as the most beneficial and trustworthy method for absolute metabolomic measurement (Alonso et al., 2014; Goldansaz et al., 2017).

2.3.2. Theoretical principles

Only nuclei with nuclear spin (\mathbf{I}) that is non-zero (I value greater than zero) are detectable by NMR (referred to as "active" nuclei). Spin, whether electronic or nuclear, is an intrinsic property of matter, as are mass or electric charge. The nuclear spin property derives from the composition of the nucleus in protons and neutrons and assumes different values according to the number of protons and the number of neutrons that make up the molecule. When $I \neq 0$, the nuclear spin gives the nucleus the property of having a nuclear magnetic moment (μ_N). Such a magnetic moment is a vector that, in the presence of a magnetic field (B_0), interacts energetically with B_0 as a result of aligning its direction with the lines of the magnetic field force, i.e., with the direction of the magnetic field (in the same way that an electric dipole aligns with the direction of an electric field). The alignment of the direction of the magnetic moment vector (μ_N) to the direction of the magnetic field B_0 , i.e., the energetic interaction between the nuclear spin magnetic moment and the magnetic field, causes the two vectors (μ_N and B_0) to assume different orientations with respect to each other, and any possible mutual orientation depends on the value of the spin (\mathbf{I}), as well as being characterized by its specific energy value, which is different for each orientation. By studying how atomic nuclei (in particular atoms such as ^1H and ^{13}C) behave in a magnetic field when they are excited by investing them with radio waves, Nuclear Magnetic Resonance (NMR) spectroscopy enables comprehensive information on the structure of molecules. The absorption of these radio waves is detected after inserting the molecule under investigation in a strong magnetic field (B_0), which results in nuclear spin transitions (i.e., in aligning the nuclear spin magnetic moment to the direction of the magnetic field).

According to the relationship, only nuclei with a nuclear magnetic moment with a non-zero spin can be observed during NMR experiments.

$$\mu = I \times \frac{\gamma h}{2\pi}$$

where (\mathbf{I}) is the quantum number of nuclear spin (which is commonly used in the same sense as nuclear spin), given by the combination of protons and neutrons that make up the nucleus; γ is the gyromagnetic ratio of the nucleus (specific to each nucleus); for hydrogen it is $26.75 \times 10^{-7} \text{ gauss}^{-1}$; h is the Planck's

constant (6.626×10^{-34} J·s). The possible values for I (quantum number of nuclear spin, or simply, nuclear spin) are the following:

i. If the protons and neutrons are even, the nucleus has a nuclear spin quantum number of $I = 0$. This is because the spins are all paired, one in opposition to the other, and cancel each other out. Nuclei of this type are not observable at NMR.

ii. If the protons are odd and neutrons are even, or vice versa, then the nucleus's I has half integers ($1/2$, $3/2$, $5/2$, etc.). An example is ^1H , with only one proton, one of the most studied nuclei at NMR.

iii. If the protons and neutrons are odd, then the nucleus has integer I (1, 2, 3, etc.).

A nucleus with a non-zero spin immersed in a magnetic field is subjected to an interaction force that makes it align its magnetic moment μ (which, in the absence of external magnetic fields, can take any direction or direction towards) with the external magnetic field B_0 . In short, it behaves like a magnetic bar.

The possible orientations that the nuclear magnetic moment (μ_N) can take when immersed in a magnetic field B_0 (Figure 1.1) are governed by a specific quantum number (m_I , quantum number of nuclear magnetic orientation), which is defined only in the presence of a magnetic field and which can take values from $-I$ to $+I$ with increments of one unit (so its values are $2I + 1$). In the case of a nucleus with $I = 1/2$ (like ^1H and ^{13}C) there are only 2 possible orientations: one with $m_I = -1/2$ (*antiparallel orientation or "spin down"*) and one with $m_I = +1/2$ (*parallel orientation or "spin up"*).

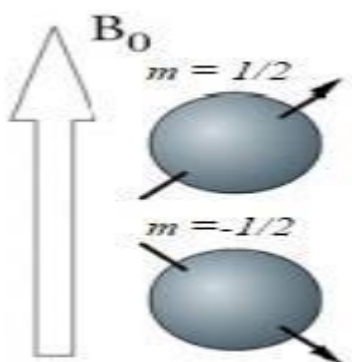


Figure 1.1. Orientations that the magnetic moment of an atomic nucleus with non-zero spin can assume when immersed in a magnetic field B_0 .

The two possible states of the nucleus do not have the same energy: the state with spin up, or ground state (direction aligned with the magnetic field), has slightly lower energy than that with spin down, or excited state (direction opposite to the magnetic field). At room temperature and with $B_0 = 0$, the population of ^1H nuclei in the two states is practically identical, with only a very small prevalence (6 protons per million) for the low energy state aligned with the field.

Due to the quantummechanical reasons related to the allowed values for I and m_I , the nuclear magnetic moment μ , unlike a commonly understood magnetic bar, does not exactly align with the direction of the magnetic field B_0 but is slightly inclined with respect to it, so it rotates around it according to a movement

called rotating precession motion (it is worthy to emphasize that it is the magnetic moment vector that rotates, not the nucleus!).

The precession motion of the magnetic moments μ occurs with a frequency called Larmor frequency (ν_0), specific for each atomic nucleus:

$$\nu_0 = \frac{\gamma}{2\pi} B_0$$

The energy difference ΔE between spin up and spin down is directly proportional to the Larmor frequency:

$$\Delta E = \nu_0 h$$

It is obvious that raising the applied field B_0 raises the ΔE between the two levels and, as a result, the Larmor frequency.

If the sample is irradiated with electromagnetic radiation of a frequency equal to that of Larmor, there will be an interaction between the magnetic component of the radiation sent and the nuclear magnetic moments, also oscillating at the Larmor frequency. The energy of the radiation is then transferred to the nuclei, which, by absorbing it, invert their spin orientation (strictly speaking, the definition of spin inversion is formally correct only for nuclei with only two possible orientations, such as the proton ^1H and the carbon ^{13}C).

In the most advanced instruments, the impulse method and Fourier transform are used to create the NMR signal. This method uses a radio frequency pulse with a frequency range of 10 MHz to 1 GHz to simultaneously stimulate all of a species' nuclei for examination. In order to better understand the phenomena underlying the NMR spectroscopy, the matter is treated on a macroscopic scale, and the macroscopic magnetization vector M_0 is thought of as the resultant vector of all the nuclear magnetic moments μ . M_0 is tiny and aligned in the Z direction with the magnetic field because there are somewhat more nuclei that are aligned with it.

Let's consider for a moment a sample made up of only one type of nucleus, such as ^1H , and irradiate the sample along a direction perpendicular to z with a radio frequency pulse that also contains the Larmor frequency of the nucleus under consideration. All ^1H nuclei are equal to each other and will absorb energy and go through a spin transition. M_0 starts a precession motion around the X axis in which the radio frequency is sent (Figure 1.2), moving away from Z axis. After a while (for instance, after a time needed to reach a plane perpendicular to Z, i.e. the Y axis in figure 1.2), the radio frequency pulse is interrupted by the operator (or by the software pulse program). The excited nuclei slowly release the absorbed energy to the nearby atoms, and the magnetization vector, making spiral oscillations around the Z axis, returns to its initial value. The signal generated during this stage of the re-emission of the absorbed energy is captured by a receiving circuit (therefore, it indirectly records the energy absorbed and then emitted by the nuclei).

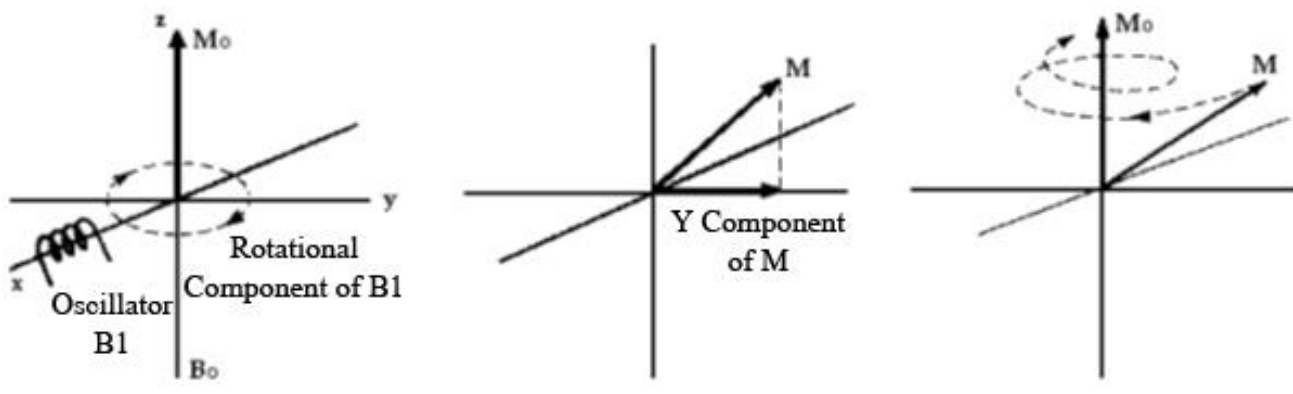


Figure 1.2. Rotation of the Macroscopic Magnetization vector M_0 in the XY plane around the z axis

The signal collected is an oscillating electric signal with a frequency equal to the Larmor frequency of the core type under examination, called FID (Free Induction Decay), which in the timeline is attenuated to zero.

By applying to the FID the Mathematical algorithm known as the Fourier Transform, we pass from a signal in the space of times to a signal in the space of frequencies (Figure 1.3), and the value of the frequency that generates the FID is obtained (for the Heisenberg uncertainty principle, the single vertical signal widens into a peak).

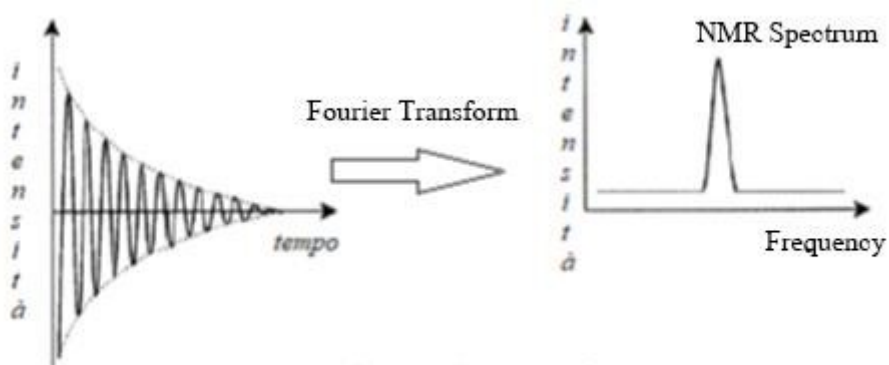


Figure 1.3. Transformation of the FID generated by a single type of nucleus into the corresponding signal in the NMR spectrum

Using the suitable radio frequency pulse, which includes the Larmor frequencies of all the nuclei present in the sample, which is the reality of things, all the sample's nuclei are simultaneously excited, giving rise to a resulting FID consisting of a complex radio frequency envelope. By applying the Fourier transform to this FID, it is possible to trace the single frequencies that, when combined, have generated the complex trace in the space of times (which is the "true" NMR signal) and thus obtain the NMR spectrum (Figure 1.4), made up of a more or less complex set of resonance peaks.

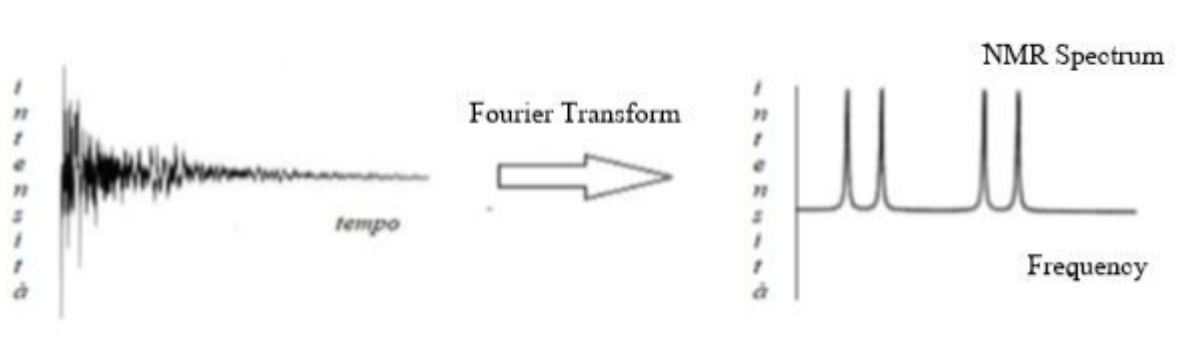


Figure 1.4. Transformation of the FID of a complex molecule into the corresponding signal in the NMR spectrum

2.3.3. Metabolic Profile Analysis (Metabolomics)

The NMR spectrum (Figure 1.5) shows the signal intensity (y axis) as a function of frequency (x axis). The various peaks correspond to the various frequencies detected, and the area they subtend is proportional to the concentration of the nuclei, generally reported not as a function of absolute frequencies (Hz) but as a function of their differences in frequency (δ) expressed in ppm (parts per million) compared to a standard (conventionally positioned at 0 ppm).

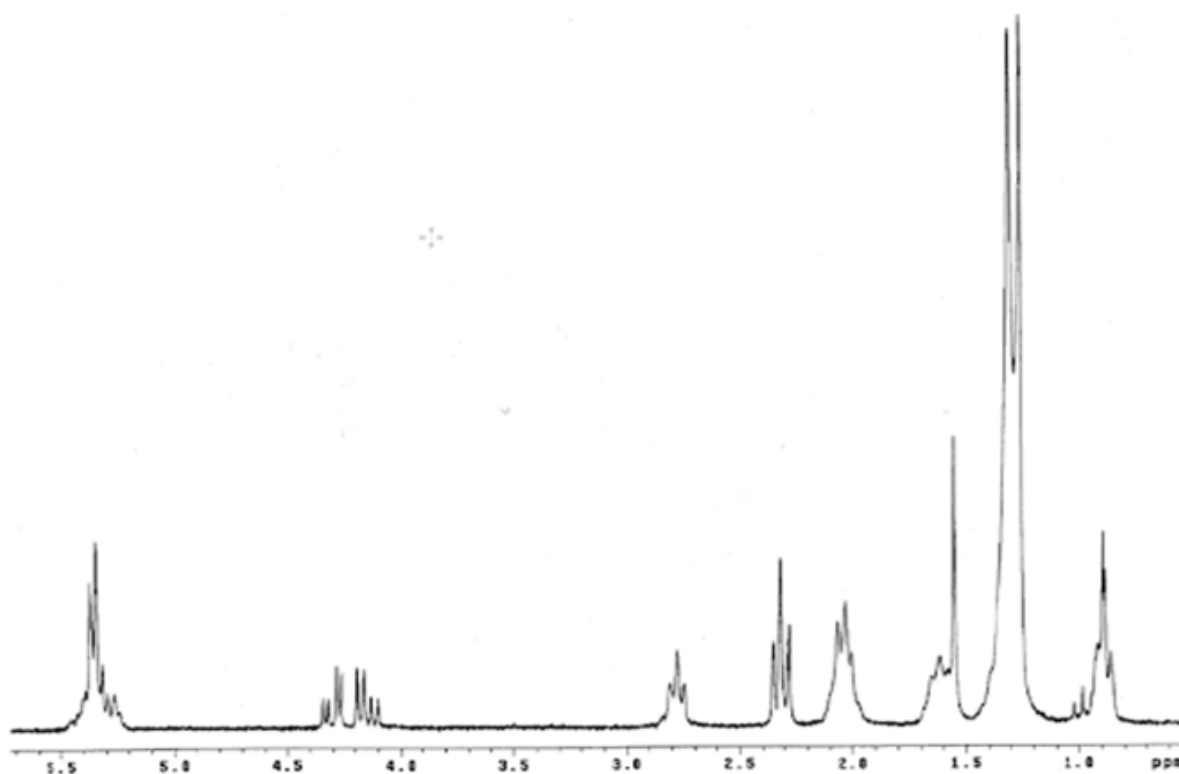


Figure 1.5. Example of an NMR spectrum

2.3.4. Statistical analysis of spectroscopic data (Metabonomic)

The use of chemometrics (a branch of multivariate data analysis that, using statistics, extracts chemical information from large multivariate data (Winning et al. 2008)) with NMR and MS data has grown in popularity during the past few years.

Among the various multivariate analyses (MVAs), including Independent Component Analysis (ICA), Principal Component Analysis (PCA), Partial Least Squares Analysis (PLS/predictions), and Hierarchical

Clusters Analysis (HCA), the most robust and helpful are PCA and PLS. The recorded NMR spectra are divided into spectral intervals of the same size, called buckets, and the value of each bucket corresponds to the area subtended by the part of the signal included in that bucket (spectral interval). A numerical data table (called a "bucket table") is created from such buckets in the sense that each row represents a spectrum or sample (a row has as many cells as are the buckets or intervals in which the spectrum was divided) and each column represents a specific bucket (meaning that each cell of the column represents the same bucket for each spectrum). Huge bucket tables with hundreds of rows and thousands of columns and correlated or uncorrelated variables can be produced.

The bucket table serves as the input information for all the statistical techniques above mentioned, but PCA and PLS provide the best and most robust performances for NMR.

Three areas of applications are important:

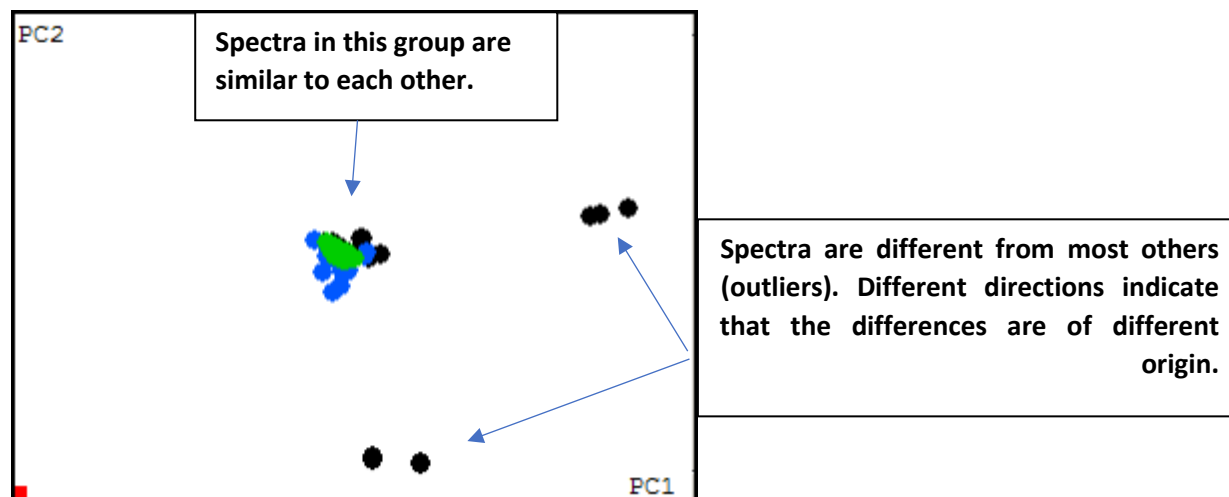
- If you have an ensemble of spectra, you want to determine whether or not all of them are comparable to one another. In order to respond to this query and identify hidden phenomena or trends by connecting them to the original variables (buckets, signals), an unsupervised soft modeling technique like PCA is used.
- An ensemble of spectra can be constructed to describe a well-defined state. This is called supervised model building because human experts control it. Other spectra can then be tested to see if they belong to the model or not. This is called classification.
- If secondary information is available for the ensemble, like other measurements, e.g., concentration values of a compound, one might be interested in relating this information with the bucket table (using regression or fitting). A robust way to do this is Partial Least Square fitting (PLS). If a good correlation can be established between the bucket table and separate measurements, the data can be used as a calibrated PLS model. The PLS model can then be used for other new spectra to predict the missing secondary information. Using descriptive data (for example, healthy and sick, blond and dark) instead of measured data as secondary data is also possible. Spectra belonging to two different groups could, for example, simply be assigned the described data 0 and 1. PLS would then find linear combinations of variables that fit well to this grouping, i.e., have a discriminating effect (PLS-DA).

2.3.5. PCA and classification

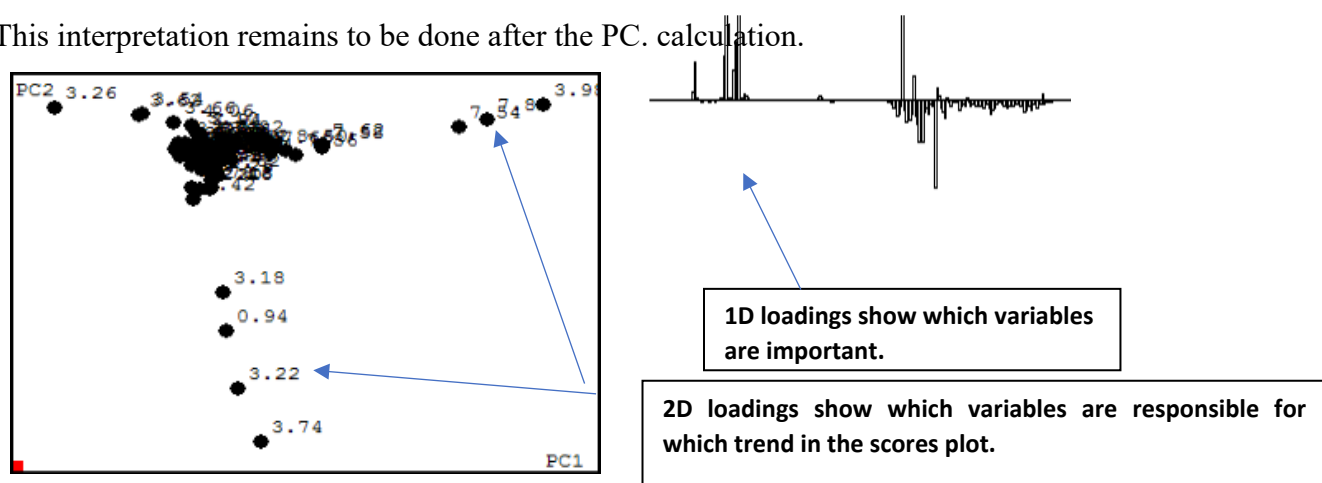
PCA (Principal Component Analysis) is the most commonly used statistical technique in NMR. The main idea of using PCA is to get insight into trends (e.g., a separation into two groups) in ensembles of spectra that would not be obvious in the usual spectroscopic representation, or spectroscopic space. The variables that span the spectroscopic space are the spectra's data points, or buckets, covering integrated data points, or peaks. If spectra contain, for example, 250 buckets, the dimension of the spectroscopic space would be 250. PCA involves a coordinate transformation from the spectroscopic space into a space that is spanned

by the principal components of the variance, which in turn are related to the directions of the largest variances in the ensemble.

The new space might have the same dimension as the old spectroscopic space, provided enough spectra are involved. It is possible to determine whether all spectra have comparable positions (scores) with respect to the relevant portion of the variance by examining 2-dimensional sub-spaces like, for example, PC₁ vs. PC₂, PC₁ vs. PC₃, etc. Score plots are what correspond to them.

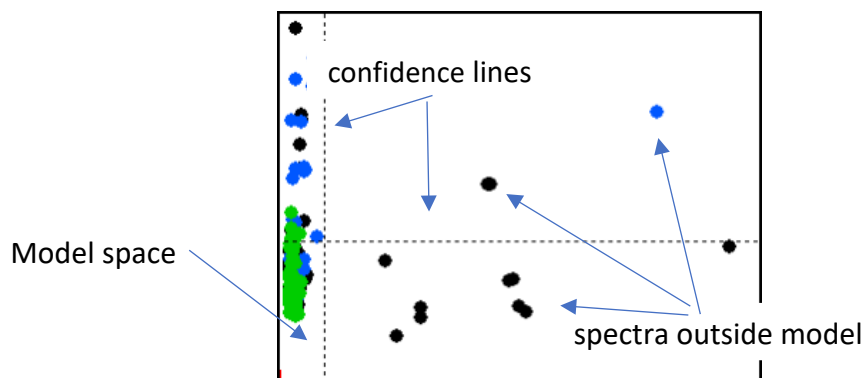


If interesting features (groups, outliers) are observed in the score's plots, one is interested in understanding the reason for this. The relation between the variables in the new Principal Component space and the original spectroscopic space is described by the so-called loadings. Studying one- or two-dimensional loading plots shows how buckets contributed to constructing the new Principal Component space. The high loading of a bucket (variable) indicates that the corresponding bucket (or peak) in the spectrum is important in determining the separation into groups or outliers. Thus, the loading plots provide the link between statistical and spectroscopic interpretation. This is essential because PCA reveals statistical phenomena but does not explain the reason for them, for example, in chemical terms. This interpretation remains to be done after the PC calculation.



Clear outliers and their causes (for instance, an unusual metabolite concentration) may be found by analyzing scores and loadings of smaller PC sub-spaces. Instead of calculating a PCA with the maximum possible number of PCs, one can select a smaller number of PCs such that only most of the variance (e.g., 99%) is explained. These PCs span a reduced variance space called model space. For each spectrum, one

can then calculate the distance to this space and the distance to the center of this space. If the distance between the model and the model center is plotted against each other and confidence lines are added, one can distinguish between spectra inside and outside the model. The corresponding plot is called the influence plot. The position of the confidence lines (and therefore the model space size) depends on the number of PCs, spectra, and confidence limits. Other spectra can be examined to determine whether or not they fall into the model space if spectra inside the model space are stored as a model (class).



Model building and classification are used in a wide range of disciplines, including chemistry, biochemistry, medicine, food analysis, material science, etc. Sometimes it can be challenging to obtain reliable results, especially when the data is complex (such as bodily fluids), and signal intensity variations are common (such as those caused by metabolites). Therefore, many applications merely use PCA or PLS-DA in a more qualitative approach to identify major trends (e.g., a separation between treated and non-treated species). A lesser number of spectra can be used to accomplish this.

2.3.5.1. PLS, PLS-DA

PLS also starts with an ensemble of spectra translated into a bucket table. In common terminology, the bucket table is now called the X table. The number of X variables is the number of buckets (the number of columns in the X table). However, a second table of information is needed. This could be other spectroscopic data or any other data, like concentration measurements, arbitrary ID numbers, etc. The Y table is the common name for this supplementary table. The number of columns in the Y table is the same as the number of Y variables, also known as response variables. Using relevant linear combinations of variables from the X table and the Y table, PLS seeks to identify the direction of maximum variance in the X table, as opposed to PCA, which looks for this direction in the X table. There is an interesting usage of PLS motivated by the following situation: Ensembles often contain different groups of spectra, say normal or abnormal, or originate from different samples, say kidney, liver, etc. One would then like to see these groups in a PCA analysis, e.g., as different clusters in a score plot. However, PCA is designed to find the maximum variance in the ensemble, not necessarily the part of the variance that results in the best discrimination. To enforce this, one can, of course, perform a spectroscopic analysis first and find signals in the spectra that would be responsible for discrimination, and then mainly use these signals in a

subsequent PCA. Alternatively, it is possible to supply a Y table containing discriminating information (in the simplest case, just 0 and 1). A PLS then detects that part of the variance in the ensemble that best fits the Y table. A score plot of the ensemble data may possibly show good discrimination. How far such a proceeding is saved or not depends on the application. If there are, for example, no two different groups in the ensemble, a PLS using a Y table with 0 and 1 will also not provide good discrimination, and the correlation plots between X and Y data would indicate poor correlation. If the ensemble, in fact, contains two groups of spectra, PLS with a corresponding Y table can indeed improve discrimination. The spectroscopic or other data should, however, confirm this; otherwise, not-well-founded discrimination could be overemphasized. Especially if the number of spectra is much smaller than the number of bucket variables, non-justified results can be enforced. It is then, for example, possible to generate two groups of spectra even if the bucket variables contain random values.

2.3.5.2. Selecting proper input variables

Any multivariate technique works on tables containing samples and variables. In spectroscopic applications, bucket tables are used. The statistical results rise and fall with the bucket tables. Using different bucketing techniques can optimize results. By eliminating variables, one can get rid of disturbing effects; by scaling rows and columns, one can change the importance of samples or variables. If such a bias is justified or critical, it depends on the individual case.

In many applications, it turns out that the combined interpretation of statistical and spectroscopic variables is of crucial importance. The reason is that the variance in the data often results from a combination of sources (e.g., chemical reasons, sample preparation, data acquisition, and data processing), and the interesting phenomena may be completely hidden. Another reason is that the results of multivariate analysis are often either trivial ("you eat fish, then a huge TMA peak in your urine makes you an outlier") or unclear ("dosage caused kidney damage, now urine becomes so different that no clear trend is visible"). Again, in many other cases, you see a trend (like splitting into two groups), but you do not understand why. One may already use spectroscopic knowledge when generating the bucket table, i.e., design the buckets such that certain influences are minimized (variable size, exclusions, etc.). The interpretation of the results needs spectroscopic and biochemical knowledge. Combining statistics and spectroscopy are major features of the statistic software used in NMR.

2.3.6. Generating bucket tables

The statistics toolkit used for this thesis (AMIX, Bruker Italia) contains all the tools needed to calculate and manage bucket tables. Tables and associated parameters are stored in user-defined folders and can also be exported to other programs if needed.

AMIX can calculate bucket tables from NMR and MS spectra. Some bucketing techniques can be applied to the spectra: rectangular bucketing, variable size bucketing, point-wise bucketing, and advanced bucketing (Figure 1.7).

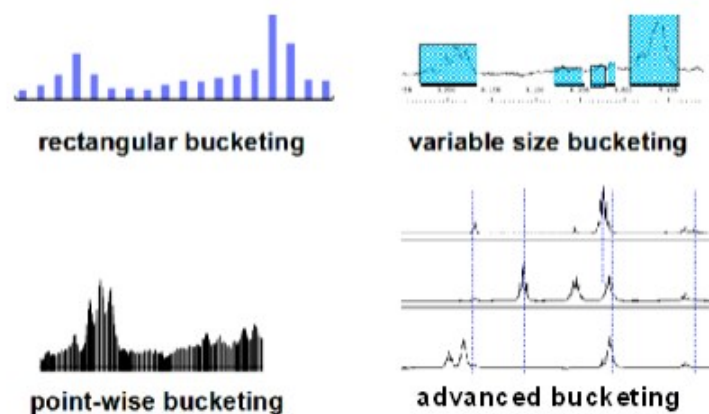


Figure 1.7. Schematic display of available bucketing techniques

2.3.7. Rectangular bucketing (1D/2D NMR, LC-MS)

The classical technique is simple rectangular bucketing. Spectra are divided into equally sized regions and integrated, e.g., point-wise. Other software packages add peak analysis and test whether a peak would cross the border of a bucket. A correction can then be made. This technique is sometimes called intelligent bucketing or kernelling. Since AMIX offers other alternatives to rectangular bucketing, kernelling is not used. Rectangular bucketing is the default method if no further knowledge exists about the spectra. It should be mentioned that fractions of points are calculated if the bucket borders (for example, defined in ppm) do not hit the data set grid points. This avoids systematic rounding problems, which have sometimes been called bucketing noise. Rectangular bucketing is certainly a compromise and may have some severe drawbacks; see the discussion about combined covariance analysis.

2.3.7.1. Point-wise bucketing (1D NMR)

Rectangular bucketing is simply a specific example of point-wise bucketing. This time, a bucket is used to represent each data point. The associated spectrum's sweep width and calibration are taken into consideration. For large line spectra, like in vivo spectra, point-wise bucketing is preferred.

2.3.7.2. Variable size bucketing (1D NMR)

Variable-sized bucketing means that each bucket may have an individual size. Internally, the buckets are handled as a spectral pattern. Consequently, one can just define a spectral pattern and use it directly for bucketing. An elegant method is, for example, to use several reference spectra (e.g., metabolites) that can be automatically compiled into a pattern. Bucketing and statistics would then focus only on the signal regions of these metabolites. The individual bucket sizes are derived from the individual line shapes of

the involved peaks in the reference spectra. Variable-sized bucketing is also the method of choice if it is known that the spectra suffer from pH changes. Signals showing larger shifts can be compiled into broader buckets than those that stay constant. The effect of signal shifts can thus be reduced significantly. To avoid additional scaling of variables due to bucket size, the integrals of each bucket can be divided by the number of data points in the bucket.

2.3.7.3. Advanced bucketing (1D NMR, LC-MS)

Advanced bucketing is a newer technique internally based on picked peaks. Although computationally intensive, there are two major advantages to this technique.

- Peaks existing in only one spectrum are stored in columns that otherwise have only zero entries. Their significance is raised.
- Advanced bucketing allows fine bucketing, e.g., in LC-MS. One may take the spectrometer's mass resolution as the bucket size. A normal rectangular bucketing would result in bucket tables with ten thousand columns, most of them useless. The advanced bucketing only creates columns if needed and reduces the table sizes.

In many applications, this truly advanced bucketing gives better results than normal rectangular bucketing. However, there are limitations and severe consequences:

- If it is known that peak positions are not well preserved and peak windows are selected at smaller than expected shifts, then bad results are obtained. In the case of NMR applications, one typically does not use advanced bucketing for urine spectra, but it is frequently used for plasma spectra.
- Bucket tables must be recalculated whenever the involved spectra change. The required logistics make this technique quite complicated, which is probably why most programs do not offer it. AMIX takes care of all necessary recalculations automatically.

2.3.7.4. Bucket table calculation with 1D NMR spectra

All bucketing techniques are offered for 1D NMR spectra.

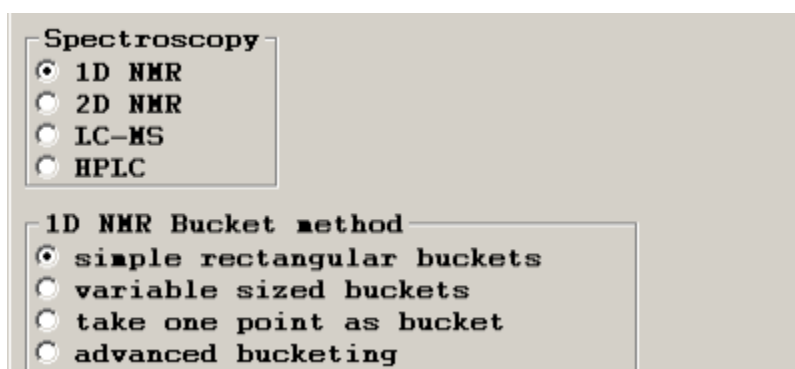


Figure 1.8. Available bucketing techniques for 1D NMR spectra

The first option would be simple rectangular bucketing.

The screenshot shows a software interface for NMR bucketing parameters. On the left, there are three input fields: 'left border (eg. 10.0)' with value '10', 'right border (eg. 0.0)' with value '0.1', and 'bucket width (eg. 0.05)' with value '0.05'. Below these are two sections: 'Integration mode' with radio buttons for 'sum of intensities' (selected), 'sum of absolute intensities', 'positive intensities', 'negative intensities', and 'special integration mode'; and 'Scaling' with radio buttons for 'scale to biggest bucket', 'scale to reference region', 'scale to total intensity' (selected), and 'no scaling'. On the right, there are 'Exclusions' radio buttons for 'no exclusions', 'edit exclusions' (selected), and 'load exclusions from file'. Below that is a text field for 'Exclusions' containing 'exclude EDTA.pa'. Further down is a 'Reference region' section with 'left' and 'right' input fields (values 10 and 1) and 'ppm' labels. At the bottom right are two checkboxes: 'check calibration (1D)' and 'check baseline (1D)', both of which are unchecked.

Figure 1.9. Bucket parameters as used for rectangular bucketing in NMR.

It must specify which spectral region should be used (left and right borders) and, very important, the bucket width. In many cases, users refer to published values. Urine spectra are, for example, very often bucketed at 0.04 ppm. Unwanted spectral regions should be excluded. Exclusion areas can be defined (edit exclusions), saved to disk after the editing, and just reloaded the next time (load exclusions from file). The integration mode would, in most cases, be the sum of intensities. Occasionally, if it is known, for example, that all artifacts in the spectrum are negative in intensity, one could select positive intensities to leave the artifacts out.

For the scaling feature, scales to total intensity are used. In this case, the bucket integrals are divided by the total spectral intensity. This (also if scale to the biggest bucket is used) can be a problem if there are huge signals (e.g., non-excluded artifacts) and very weak signals in the spectrum at the same time. In extreme cases, weak signals could disappear. Scaling to a reference region would be best if such a region could be defined. Not applying any scaling is only recommended in cases where sample concentration and experimental parameters are identical for all spectra.

Another option is called check calibration. Users relied on well-calibrated spectra (that is the reference peak exactly located at 0 ppm), but then got unexpected statistical results because of small calibration errors. AMIX can check the calibration in the case of 1D NMR (and LC-MS spectra). You must specify a peak at the calibration position. If such a peak is not found at the expected position, the spectrum can be color-coded during PCA (to avoid it getting overlooked), the bucketing can be aborted, or the result can just be ignored. Finally, there is an option called check baseline. Spectra should be well baseline corrected, but it is often overlooked that the baseline is not at 0 but different in different spectra. This causes additional variance. The check baseline option checks if spectra have a baseline that is not equal to zero.

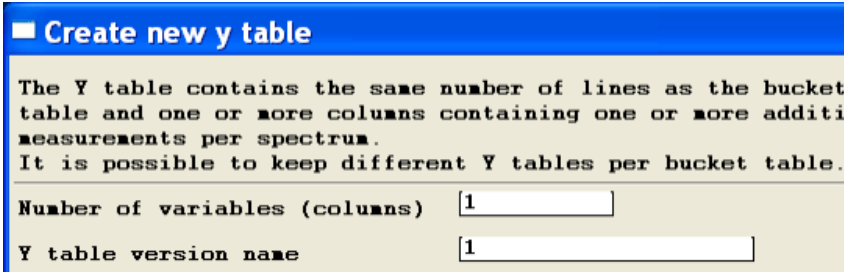
The following sheets of the wizard relate to the selection of spectra which shall contribute to the table. Spectra should either be stored in a normal personal computer path or should be described in a project. Spectra names are defined and selected.

Generally, the selection of the spectra is often split into two or more steps. The reason to split the spectrum selection into pieces is to introduce groups in the spectra ensemble. Each round of selection defines another group of spectra. This may be interesting if such groups are essential for the statistical analysis later.

2.3.8. Generating other tables (Y table)

A PCA analysis only needs a bucket table, but a second table is needed when using PLS. In common terminology, the bucket table is called the X table, and the secondary table is called the Y table. The Y table contains additional data for each of the spectra contained in the X table. Several options exist to generate a Y table.

The table(s) must reside in the same directory as the bucket table. One has to specify the number of variables and the name of the Y table. The first column of the Y table is identical to the first column of the X table and contains the short names of each of the spectra. The first row of the Y table is a dummy row (bucket tables and Y tables thus have the same format). This was prepared by AMIX. Then, a number of columns follow according to the number of variables you specified. These columns must be filled out by the operator.



■ Create new y table

The Y table contains the same number of lines as the bucket table and one or more columns containing one or more additional measurements per spectrum.
It is possible to keep different Y tables per bucket table.

Number of variables (columns)

Y table version name

Figure 1.10. Generating a new Y table.

Frequent usage of PLS is PLS-DA. In this case, the Y table does not contain independent physical measurements but just numbers that express that the spectra belong to a certain group. If you have, for example, two groups of ten spectra each, then ten spectra could have 0 in the Y table, and the other ten spectra could have 1 in the Y table. If you have already generated your bucket table group-wise, the corresponding group ids already exist, and AMIX asks whether to use them directly as entries in the Y table.

2.3.9. PCA

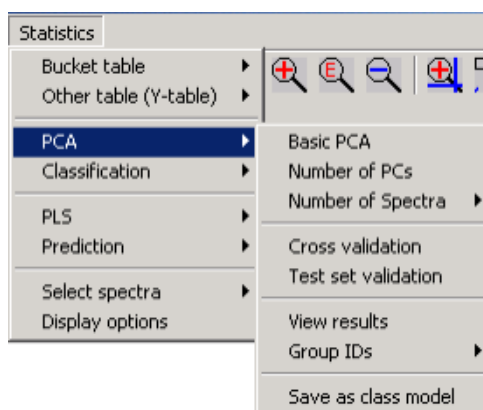


Figure 1.11. Commands related to PCA.

2.3.9.1. Basic PCA

After a bucket table has been calculated or loaded, principal component analysis can be applied. Some details have to be specified. The first option is about the scaling of columns in the bucket table.

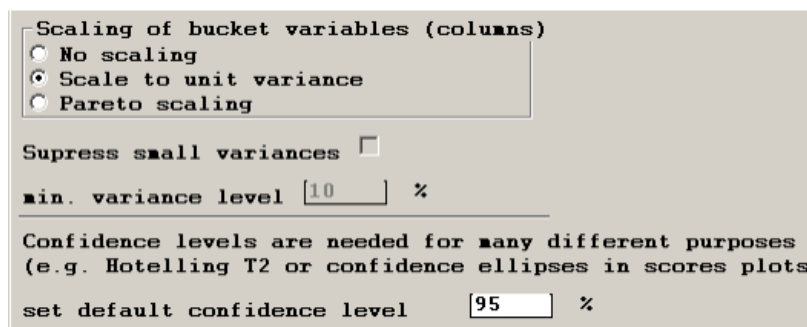


Figure 1.12. Scaling of columns prior to PCA calculations

Explanation:

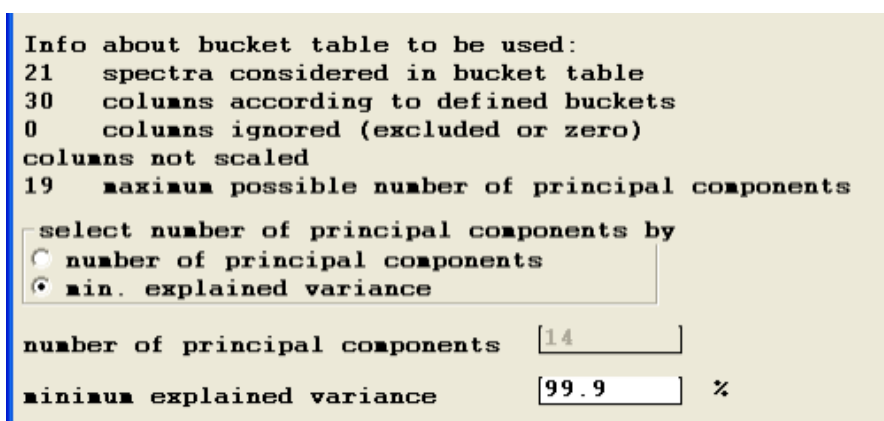
The bucket table rows should be scaled so that spectra produce comparable buckets. This is done during bucket table calculation; typically, a scale to total intensity is used. The columns (variables) of a bucket table can also be scaled. This has a dramatic influence on the PCA results. Some software packages, by default, scale the columns to unit variance. This means that all columns are equally weighted during PCA. This scaling is, for example, needed if the variables are not measured in the same units and have very different absolute numbers, which in turn can cause large variances. This would falsely dominate PCA. If the variables are comparable (typically the case for NMR or MS buckets), no scaling is often better. It preserves natural differences in intensities, and it highlights dominant effects. For example, an unexpected metabolite in body fluid can be more clearly identified in the loadings plot. Pareto scaling has an impact on the PCA results between no scaling and unit variance scaling.

The second option is handling small variances only if "no scaling" has been chosen. Columns in the bucket table containing almost constant (and small) values do not produce a large variance and would not significantly influence the PCA. If there are many of them (especially in LC-MS applications), loading plots get crowded and hard to read. Suppressing small variances would help. Variables that do not

produce a certain minimum variance (given as a percentage of the maximum variance) are removed from the PCA calculation.

The third option is about confidence levels. Confidence levels are needed for several purposes, e.g., if confidence ellipses are drawn into the score plot. Given a gaussian distribution of dependent variables, such ellipses indicate an area around the mean. With a probability that equals the confidence limit (e.g., 95%), spectra are inside this area if they belong to that gaussian distribution. Confidence levels are also used in hotellings and influence plots.

The second dialog window prior to PCA deals with the number of PCs to be used. One can either define an absolute number, e.g., ten, or let the program calculate the number such that a certain amount of the total variance (e.g., 99%) gets explained.



```
Info about bucket table to be used:
21  spectra considered in bucket table
30  columns according to defined buckets
0   columns ignored (excluded or zero)
columns not scaled
19  maximum possible number of principal components

select number of principal components by
 number of principal components
 min. explained variance

number of principal components  [ 14 ]
minimum explained variance     [ 99.9 ] %
```

Figure 1.13. Selecting the dimension of the model space.

The number of chosen PCs is irrelevant for a simple qualitative analysis in which one just checks some major score plots. The score plot of PC1/PC2 remains the same no matter if PCA is calculated with 10 or 20 PCs. But as soon as modeling is an issue and things like distance to model, confidence regions, etc., are to be considered the number of PCs is important. If the number of PCs is chosen as high as possible, all spectra are regarded as belonging to a big model, which generally makes no sense. Thus, the number of PCs chosen is that one sufficient to explain 99% or 99.5% of the total variance.

2.3.9.2. Some remarks

The time needed for the PCA calculation depends on the bucket table size. The covariance matrix is calculated, and all eigenvectors and eigenvalues are obtained simultaneously via SVD (singular value decomposition). The calculation is finished quickly with small tables (a few dozen spectra, 200 buckets). Large tables (more than 1000 spectra, more than 10,000 buckets) may take considerable time. Such huge tables may occur in LC-MS applications. After the calculation is finished, the types of plots which will be displayed can be selected (Figure 1.14).

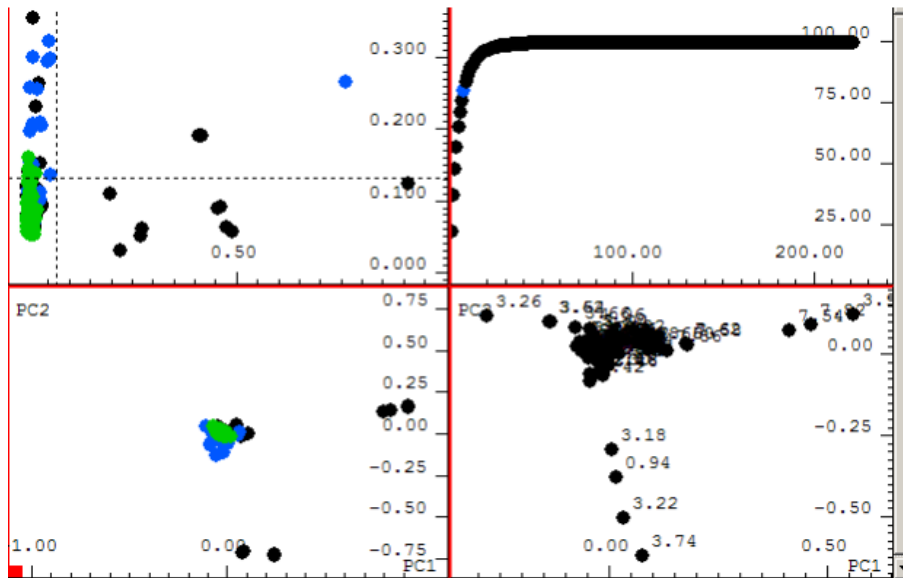


Figure 1.14. Typical display after a PCA calculation

```

influence plot 
hotelling's t2 plot 
explained variance 
scores 
2D loadings 
scores and loadings
   in new window
   replace current

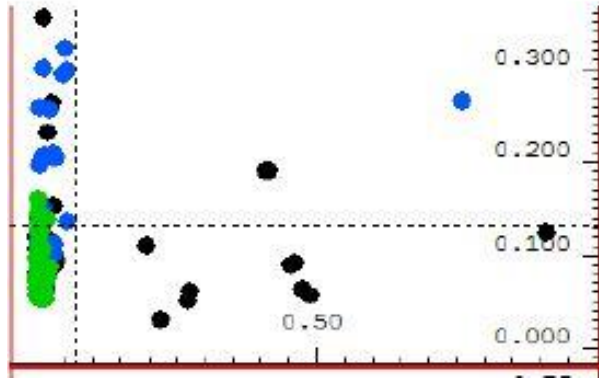
predefined plots
PC 1 vs. PC 2 
PC 3 vs. PC 4 
PC 5 vs. PC 6 
PC 7 vs. PC 8 
PC 9 vs. PC 10 
select other PC 
e.g. 5 6, 7 9, 12 32
pc 
1D loadings of PCs 
e.g. 1, 2, 3

```

Figure 1.15. Definition of the PCA display

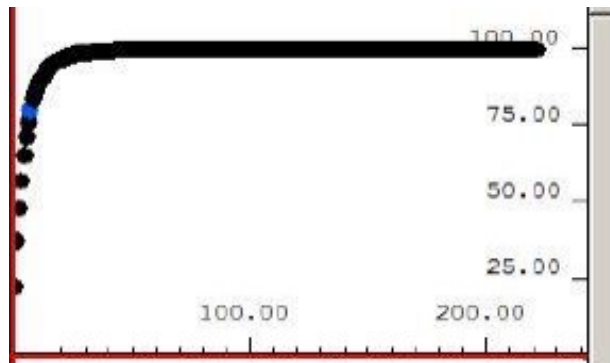
Influence plot:

Shows spectra in a diagram where the vertical axis measures how far away a spectrum is from the model space (off-model distance). If a spectrum is in the upper part of this display, it is most likely not in the model space. The horizontal axis measures how far away a spectrum is from the model center after being projected into the model space. If a spectrum appears on the right side, it strongly influences the model. The two lines displayed inside the plot are so-called confidence limits. Spectra inside these limits (the lower left area in the plot) belong to the model with a probability of, e.g., 95%. The confidence limit can be set during the basic PCA command.



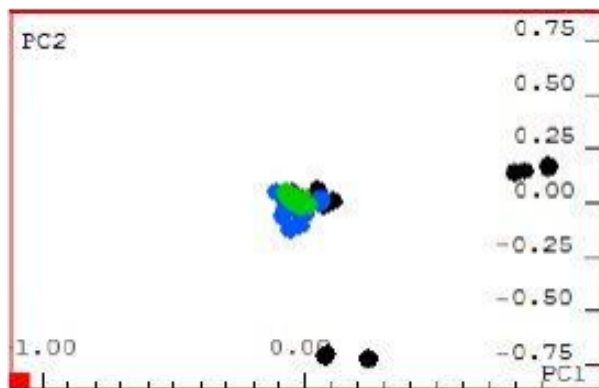
Explained variance:

This shows how the explained cumulative variance gets larger as the number of PCs increases (horizontal axis). The number of PCs that have been chosen should be such that the last PC is somewhere in the flat asymptotic part of this curve.



Scores plots:

2D score plots of the form PC_i vs. PC_j (e.g., PC_1 vs. PC_2) show how the spectra are distributed in the corresponding sub-space. This type of plot is used to see whether spectra are gathered in groups or are outliers. Dominant effects in the PCA may typically be seen in plots that involve the first few PCs. Sometimes effects on higher PCs are equally important. They could, for example, indicate strong unexpected signals in a spectrum but occur only in very few spectra. By checking the influence plot or all scores plot, it can be seen whether higher PC score plots should be looked at.



Loadings plot:

Shows how the principal components are related to the original buckets. The 1D loading plot of a principal component looks like a 1D spectrum (see figure 1.16 panel A). Peaks indicate those buckets (and therefore spectral regions) that contributed significantly to that principal component, and the largest peaks indicate the strongest contributions. 2D loadings plots (see Figure 1.16 panel B), e.g., of PC1 and PC2, relate the loadings of the corresponding two PCs to each other. Each point in such a plot corresponds to a bucket.

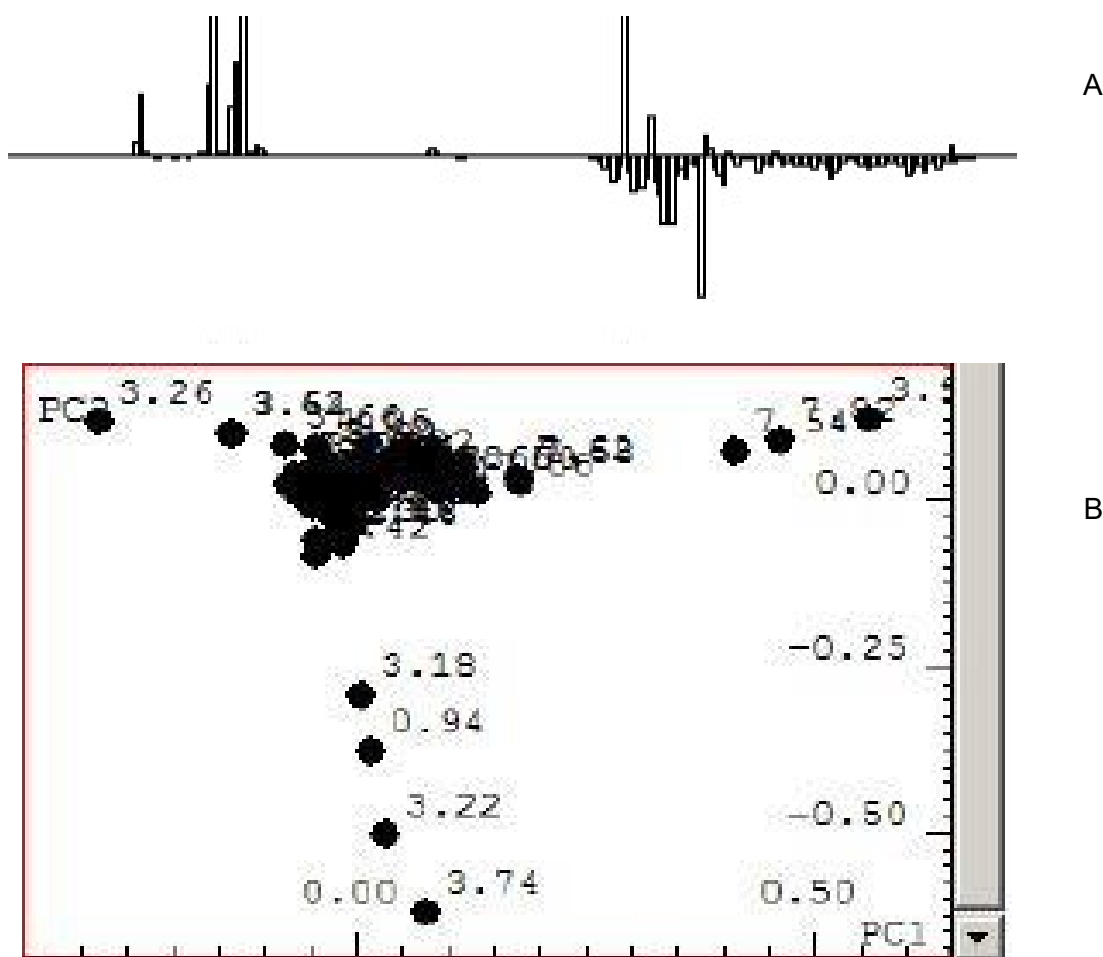


Figure 1.16. Loadings Plot 1D (panel A) and 2D (panel B).

A combined interpretation of scores and corresponding loading plots can show which buckets are responsible for an outlier behavior. Combined interpretation means looking for spectra outlying along a certain direction in the scores plot and for loadings lined up along the same direction in the corresponding loadings plot.

Figure 1.17 shows a spectrum extending along a solid arrow to the lower left. Some loadings point in the same direction. They indicate resonances which are the reason why this spectrum is outlying. A similar example with the dashed arrow.

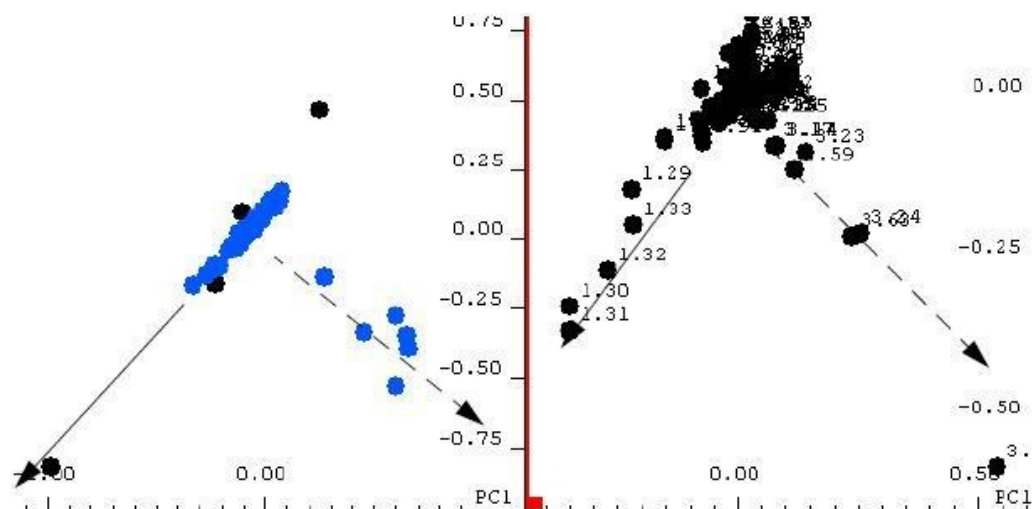


Figure 1.17. Interpretation of 2D scores/loadings plots

Hotelling's T2 Plot

The Hotelling T2 ellipse assumes a gaussian distribution of bucket variables and indicates a confident region. Within the given confidence limit (e.g., 95%), spectra inside the ellipse belong to a distribution with a mean at the ellipse's center. The user can set the confidence limit when executing the Basic PCA command. If the bucket table was calculated with three groups, for example, these three groups may be shown with different colors, and a confidence ellipse may be calculated for each group individually (Figure 1.18).

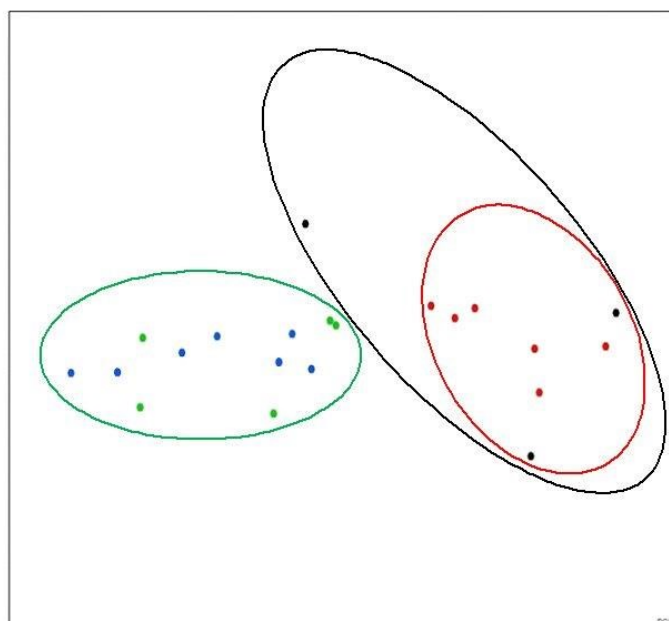


Figure 1.18. Hotellings_Plot_T2_with_Confidence_Intervals_Ellipses

If the number of spectra per group is relatively small, the confidence ellipses become very large (the radii of the ellipses are related to F-statistics, which depend on the number of spectra and degrees of freedom). The user may have lower confidence levels, e.g., 80%. Using the “show extended view (3D)” option creates a second window with a 3D score plot (Figure 1.19). The next higher PC is included, e.g., PC1 vs. PC2 extends to PC1 vs. PC2 vs. PC3. It is sometimes quicker to check higher PCs than to select more 2D score plots. If the 3D score plot is on screen, it also offers a popup menu and allows, for example, to display the Hotellings T2 ellipse for better orientation.

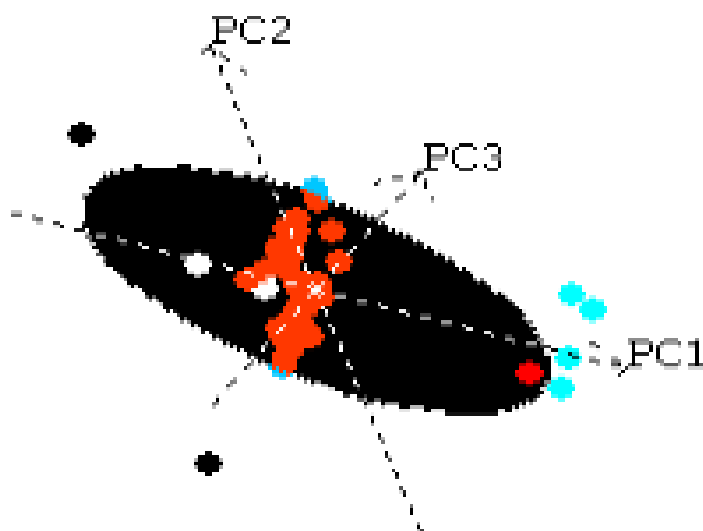


Figure 1.19. 3D scores plot with Hotellings T2 ellipse.

2.4. ¹H-NMR: metabonomic analysis

" Omics " sciences are defined as all those disciplines that allow the production of a remarkably high number of data useful for the description and interpretation of the biological system studied.

Metabolomics is an experimental approach that aims to identify and quantify all the metabolites present in a cell, tissue, or organism, making it possible to have a full understanding of the metabolic balance of a living system. This is analogous to the meaning of the other "omics" disciplines (genomics, proteomics, lipidomics, etc.).

Therefore, the quantitative and qualitative analysis of all metabolites present in a fluid or biological tissue is known as metabolomics (metabolome). The very dynamic nature of the metabolome, which makes it a very quick and effective indication of disturbances in a system, is a key characteristic of the metabolome (Bremer, 1983).

Metabonomic, unlike metabolomic, concentrates on metabolic reactions as a result of pathophysiological stressors, and on the consequent variation of the metabolic profile of the biological fluid under investigation.

An organism responds to any pathological state, inducing, among others, disturbances of its metabolism. Starting from this principle, Metabonomic deals with identifying any correlation between metabolic variations and causes through a comparative analysis of the metabolic spectra typical of the physiological

state and the pathological state. Changes in metabolic profiles and their distribution can be viewed as a reflection of a biological system's *in vivo* biochemical state.

Therefore, the goal of metabonomics is to assess the statistically significant changes between the metabolic profiles of organisms in physiological conditions and in a pathological state, given that the individuality and/or concentration of the metabolites produced in the two conditions differ.

As a result, the ultimate purpose of metabonomics is to identify the metabolic profile of a particular pathology in order to model and diagnose it. To better understand how a metabonomic approach differs from a metabolomic one, an example could help. If we consider mastitis, it causes an influx of several metabolites into milk in addition to altering the protein profile (Hogarth et al., 2004). It is not yet known, though, whether they are created by invasive bacteria, immune system cells, enzymatic reactions, or if they are transferred from the blood due to the alteration of the permeability of the blood-mammary barrier. It is believed that this phenomenon affects the characteristics of milk and that it is linked to a rise in the number of somatic cells in the milk. According to the literature (Sundekilde et al., 2013), detecting variations in the quantities of specific chemicals will be feasible by contrasting the metabolic profiles of two animals, respectively, with high and low numbers of somatic cells.

Butyrate, β -hydroxy-butyrate (BHB), isoleucine, lactate, and acetate are found to increase in a subject with increased SCC, although lactose, fumarate, hippurate, and citrate seem to decrease. The opposite, however, happens with animals that are healthy and have few somatic cells. The metabolic profile of milk can be useful for the assessment of other factors and pathologies in addition to this solely diagnostic aspect. For example, β -hydroxybutyrate, phosphocholine, and glycerophosphocholine can be used as biomarkers for ketosis (Klein et al., 2010). Citrate, the N-acetyl carbohydrate group, lecithin, and trimethylamine can be indicators of milk quality. Also, choline, carnitine, citrate, and lactose reflect its coagulation capacity.

The use of $^1\text{H-NMR}$ for metabolomic analysis has proven to be a beneficial method for conducting studies on milk products as well. Its application has been helpful in the control and traceability of Italian buffalo mozzarella (Mazzei and Piccolo, 2012), in the analysis of ingredients in infant formula, and in the identification of milk adulterated with melamine, a substance used to mimic an increase in protein concentration (Lachenmeier et al., 2009; Sundekilde et al., 2013). The ability to study many food products "as they are" with only a minimal amount of preparation opens the door to various applications that enable carrying out checks, quality analysis, and origin determination—factors that are challenging to certify with other techniques but are in increasing demand.

2.5. ICP-OES Applications

The ICP-OES technique can evaluate the metal content in a wide range of sample types, which contributes to its versatility in addition to the vast number of elements that can be quickly detected at trace levels.

2.5.1. Agricultural and Foods

The ICP-OES technique has been used to analyze a wide range of agricultural and food components. Soils, fertilizers, plant materials, feeds, foods, animal tissues, and bodily fluids are examples of sample types. It is necessary to analyze these materials to identify their amounts of harmful components as well as important nutrients.

Many agricultural and food products are often neither readily soluble in distilled water nor in the form of diluted aqueous solutions. Therefore, rigorous sample preparation procedures must frequently be carried out before analysis when using ICP-OES to analyze these components. For the analyst's benefit, modern microwave sample digestion methods are making it faster and sometimes easier to prepare samples of agricultural and food products, as well as many other sample types.

2.5.2. Biological and Clinical

ICP-OES has developed into a key instrument in the field of biological and clinical applications as research continues to shed light on the functions and behaviors of trace elements in biological systems. Essential, toxic, and therapeutic trace element determinations by ICP-OES are critical in clinical and forensic laboratory environments as well as medical research labs.

2.6. GENERAL CHARACTERISTICS OF ICP-OES

2.6.1. Detection of Emission

Plasma is a physical state of matter (sometimes referred to as the fourth state of matter) consisting of a dense ionized gas at extremely high temperature, constituted by neutral atoms, radicals, positive ions, and electrons. It can conduct electricity and is influenced by magnetic fields, which are two properties of plasmas. Ionized gases with a high energy level make up the electrical plasmas used in analytical OES. Although some research has also been done using reactive gases like oxygen, they are often created in inert gases. These plasma discharges are used to excite and/or ionize the atoms for atomic and ionic emission since they are far hotter than flames and furnaces and can dissociate practically any kind of sample. The argon-supported inductively coupled plasma (ICP) is the most advanced plasma source currently available for analytical optical emission spectrometry. The microwave-induced plasma (MIP) and direct current plasma (DCP) are two other plasmas that are now in use.

In ICP-OES, information about the sample is gathered by measuring the light emitted by the excited atoms and ions introduced in the plasma. The emission from plasma is polychromatic because the excited species present in it produce light at a variety of wavelengths specific to each atom and ion. In order to identify and measure the intensity of each excited species' emission without being hampered by emission at other wavelengths, this polychromatic radiation must be divided into its component wavelengths. A monochromator, which separates light at a single wavelength at a time, or a polychromator, which may separate light at multiple wavelengths simultaneously, are typically used to separate light according to

wavelength. After being separated from other wavelengths, the light is detected using a photosensitive detector like a photomultiplier tube (PMT) or more sophisticated detecting techniques like a charge-injection device (CID) or a charge-coupled device (CCD).

2.6.2. Extraction of Information

It is typically simple to extract both qualitative and quantitative data from a sample using ICP-OES. Finding the presence of emission at the wavelengths corresponding to the constituents of interest is necessary to obtain qualitative information, or what elements are present in the sample. To confirm that the observed emission can be accurately identified as coming from the element of interest, it is typically necessary to see at least three of the element's spectral lines. This is because the presence of an element in the plasma may occasionally be questioned due to spectral line interference from other elements. Thankfully, the majority of elements have a relatively wide number of emission lines available, which makes it possible to choose from a variety of emission lines for the element of interest to avoid these interferences. Standard solutions, or solutions containing known quantities of the target elements, are introduced and analyzed in the ICP, and the intensity of the characteristic emission for each target element, or analyte, is measured. These intensities can then be used to create a calibration curve for each element: they are graphs of emission intensity vs. concentration (Figure. 1.20), and then the emission intensity of an analyte is compared to the emission calibration curve for that element to calculate the concentration that corresponds to that intensity.

The elements that are commonly determined by ICP-OES are the metals (alkali and alkaline-earth metals, and transition metals), although some semimetals are also identifiable (for example, As and Si) as well as some nonmetals (for example, P, Cl, and Se). Depending on their concentration, macro elements are generally considered those with concentrations greater than $100 \mu\text{g g}^{-1}$, while micro elements are those with values between $0.1 \mu\text{g g}^{-1}$ and $100 \mu\text{g g}^{-1}$, and trace elements are those with concentrations less than $0.1 \mu\text{g g}^{-1}$. Moreover, some of them are included in the group of minerals (Ca, P, Mg, Na, K and S as macro elements; Fe, Mn, I, Zn, Cu, Cr, Mo and Se as micro elements), that are essential for the growth and development of humans (Chen et al., 2020), while others are grouped as toxic elements (like Hg, Cd, Cr, Ni and Pb), also referred to as heavy metals.

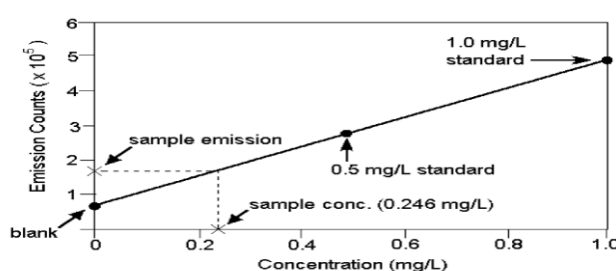


Figure 1.20. Calibration curve used for ICP-OES.

ICP-OES calibration curves are typically linear over four to six orders of magnitude; therefore, only one or two standard solutions and a blank solution generally need to be measured in order to calibrate the ICP instrument. Unlike ICP-OES, Atomic Absorption (AA), which uses arc or spark sources instead of plasma, needs five or more standards for each element due to nonlinear calibration curves. What causes nonlinearity in ICP-OES is the self-absorption mechanism, which involves some of the analyte's radiation being absorbed by ground-state atoms in the plasma. In conventional ICPs, nonlinearity in the calibration curves is typically only seen at high analyte concentrations or at concentrations that are more than 5 to 6 orders of magnitude above the detection limit.

2.6.3. Performance Characteristics

There are several elements that can be determined using the ICP-OES technique. The range of $\mu\text{g/L}$ (ppb) is where these elements' detection limits often occur. The detection limit is regarded as the lowest concentration at which the analyst may be reasonably assured that an element is present in a sample, as is the case with many procedures. However, measurements at or close to the detection limit are not regarded as quantitative. It is indicated that an element's concentration be at least five times greater than the detection limit for purposes of rough quantification (10%). The concentration needs to be more than 100 times the detection limit for precise quantification (2%). It is worthwhile to speak about the elements that are typically not determined at trace levels by ICP-OES. The components that are naturally entrained into the plasma from sources other than the initial sample fall under this category. For instance, it would be worthless to attempt to identify traces of argon in a sample using an argon ICP. Due to the common CO_2 contamination of argon gas, a comparable restriction might be faced. H and O would not be appropriate elements when using water as a solvent, while C would not be appropriate if using organic solvents. Apart from these four elements (O, H, N, and C), the majority of the over 70 elements that can be detected by ICP-OES have low detection limits.

Therefore, for the majority of trace elemental tests, the ICP-OES analyses' precision and accuracy are thought to be sufficient. Modern signal compensation techniques enable the analyst to do studies with amazing accuracy, even when there are interferences. When the concentration is greater than 100 times the detection limit, the precision of the analysis is often in the 1% or less RSD (relative standard deviation) range. Better precision can be achieved, but frequently at the expense of speed, flexibility, or both, or by taking longer measurements and using specialized signal compensation methods.

2.7. Comparing ICP-OES against other methods

Numerous methods, including flame and graphite furnace atomic absorption spectrometry (FAAS and GFAAS), atomic fluorescence spectrometry (AFS), inductively coupled plasma optical emission spectrometry (ICP-OES), and inductively coupled plasma mass spectrometry (ICP-MS), have been used to identify the elements in milk, milk-based products, ruminal fluid, serum and plasma. Using GFAAS,

Tajkarimi et al. (2008) examined the presence of lead in milk. The amount of Ca and Mg in dairy products has been established by FAAS (Brandao et al. 2011). The authors only analyzed a small number of elements because repeated sample injections are needed for multi-element analysis using FAAS and GFAAS. ICP-OES and ICP-MS are more suited for multi-element analysis as compared to other analytical techniques. Benincasa et al. (2008) employed ICP-MS to examine 16 elements in cow and buffalo milk, while Güler (2007) used ICP-OES to examine 24 minerals in goat milk and yoghurt. ICP-OES has a lesser sensitivity than ICP-MS; as a result, it is more challenging to study trace elements like Cd with ICP-OES. ICP-MS has a number of benefits, including quick operation, quick scanning, high sensitivity, a low detection limit, and a wide linear range. ICP-MS has thus become a popular tool for analyzing trace components in food.

For a given set of circumstances, choosing between the ICP-OES, FAAS, GFAAS, and ICP-MS procedures is typically not a difficult process due to their numerous benefits and drawbacks. For instance, FAAS is frequently the technique of choice when an application calls for single element trace studies for only a small number of samples or where initial cost is the most crucial aspect. The GFAAS technique would likely be chosen if an application required very low detection limits for only a few elements. ICP-MS would be a plausible contender, however, if an application required very low detection limits for 40 elements per sample. ICP-OES may be the best option if the application needed multielement analysis of materials in a complex matrix or if a high sample throughput rate with moderate sensitivity was necessary.

2.8. Clay Minerals

2.8.1. Properties

The health, productivity, and safety of livestock animals, as well as the safety of their products, can be affected by the contamination of feeds with microbiological or toxicological substances. Reducing their gastrointestinal absorption as an alternative to treating feedstuffs to reduce the concentration of undesirable chemicals before feeding is considered a preferable practice because doing so is less costly and labor-intensive. The use of clays and clay minerals is appropriate for this purpose thanks to their large specific surface area, adsorption capacity, low or zero toxicity for animals, and low cost. Various feed additives are available. It is challenging to properly categorize the enormous variety of clays available to producers because their structures vary and depend on the source of their mining. Due to their unique ability to adsorb various feed mycotoxins, clay minerals play a significant role in animal production, as seen by the decrease in diarrhea, improved feed conversion ratio, and enhanced health of many livestock species. Due to their advantageous properties, lack of primary toxicity, and success in studies to lower animal disease, improve animal productivity, and increase the safety of animal products, clays are becoming more and more popular (Nadziakiewicz et al., 2019).

Because they require a lot of effort and money, treatments that reduce the contamination of feedstuffs with mycotoxins and fungi before feeding are frequently not practical. Due to this, using various feed additives, also known as mycotoxin adsorbents or binders, to stop their absorption from the digestive tract is one of the most practical ways to reduce the negative impacts of mycotoxins in livestock diets (Peng et al., 2018; Vila-Donate et al., 2018). For their high specific surface area, adsorption capacity, cation exchange capacity (CEC), thixotropy, colloidal properties, favorable rheological characteristics, swelling capacity, dispersity, chemical inertness, low or zero toxicity for the animal, and low cost, clay minerals are the primary minerals used in animal nutrition (Al-Ani and Sarapaa, 2008).

2.8.2. Mineral Structure of Clays

A mineral is an element or chemical substance that has developed as a result of geological processes and is typically crystalline (Al-Ani and Sarapaa, 2008). They developed under certain circumstances that had an impact on their structure and characteristics. The most prevalent class of rock-forming minerals, including clays, are aluminum-silicon-oxygen-containing minerals, or aluminum silicates. The combination of silica tetrahedral and aluminum octahedral sheets, both with oxygen and hydroxyl groups, makes up the fundamental structural component of silicate clay minerals (Gregorio et al., 2014). Due to the possibility of related minerals and impurities such as quartz, cristobalite, alunite, iron oxides, anatase, magnesite, serpentine, and others, the definitions of clay minerals are still not universal (Rautureau et al., 2017). Primary materials are often generated from igneous or metamorphic rocks and are created at high temperatures and pressures. Some of them produced more stable secondary minerals. Phyllosilicates are the name given to these secondary minerals because of their platy or flaky appearance (Barton and Karathanasis, 2002). Clay minerals have various physical and chemical features (particularly the distribution of negative and positive charges on surfaces, the kind of bonds between atoms and molecules, the type of ions, and their exchangeability). There are two distinct varieties of phyllosilicates: 1:1 layer type (T-O; Figure 1.21), which consists of a sheet of SiO_4 tetrahedra linked to a sheet of Al- or Mg-octahedra; and 2:1 layer type (T-O-T; Figure 1.22). This latter type has an Al- or Mg-octahedron sheet between two sheets of Si-tetrahedra (Al-Ani and Sarapaa, 2008). The kaolinite group represents the minerals in the 1:1 layer, while the mica, talc, and smectite subgroups represent the minerals in the 2:1 layer. They have many characteristics that may affect how they are used. The term "shrink-swell potential" is frequently used to describe this smectite characteristic. In contrast, the 2:1 layers are tightly bound together in vermiculites due to the strong bonding of the interlayer cations, which prevents the basal spacing from expanding (Barton and Karathanasis, 2002). There is a second class of phyllosilicates known as the 2:1:1 layer type, which has an interlayer brucite (with cations Mg^{2+} or Fe^{2+}) or gibbsite (with cations Al^{3+}) sheet with a basic 2:1 structure. Chlorites are a member of this group. They are regarded as nonexpansive minerals since there is no water adsorption in the interlayer space (Sun et al., 2009).

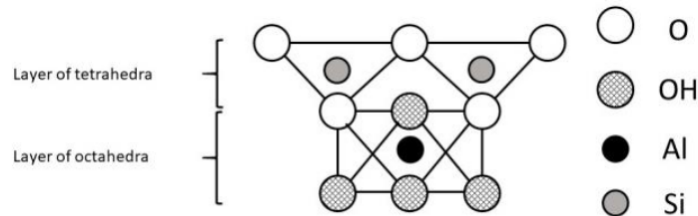


Figure 1.21. The 1:1 layer phyllosilicate structure.

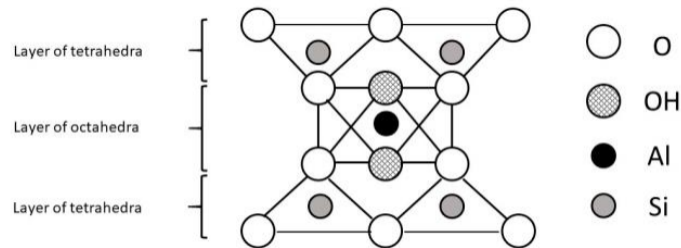


Figure 1.22. The 2:1 layer phyllosilicate structure.

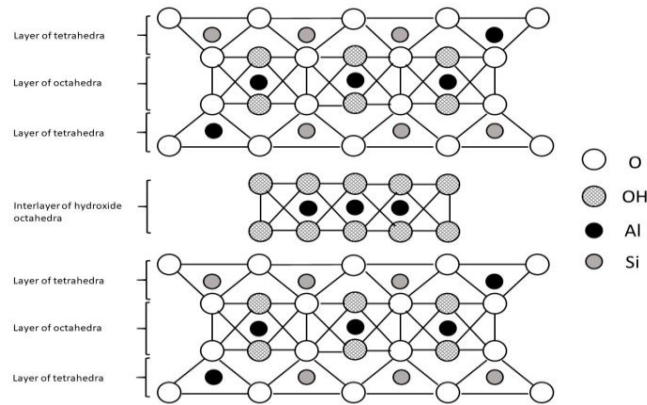


Figure 1.23. The 2:1:1 layer phyllosilicate structure.

2.8.3. Bentonite

The clays that form bentonite, which is primarily made up of montmorillonite (MMN), are strongly colloidal and plastic (Parker, 1998). The exchangeable cations found in the smectite group of minerals are readily replaced by other cations, allowing for the creation of sheet surfaces with absorbing properties. Reversible replacement is possible for these cations. Bentonite comes in two varieties: sodium bentonite, which has a single water layer with exchangeable ions (Na^+) (with swelling properties), and calcium bentonite, which has a double water layer with exchangeable ions (Ca^{2+}) (a non-swelling mineral). Bentonite may create thixotropic gels and can absorb a lot of water, increasing in volume 12 to 15 times in the process. The primary bentonite component, montmorillonite, has a high cation exchange capacity that is not greatly impacted by particle size (Adamis et al., 2005).

2.8.4. Bentonite as a food additive for livestock

Various clay minerals are used widely as non-nutritional additives in the diets of farm animals around the world, including cattle, small ruminants, pigs, chickens, turkeys, ducks, fish, and minks (Barrientos-Velázquez et al., 2016). These additives are used to homogenize the diet (prevent the formation of clots), improve efficiency, and adsorb mycotoxins (Kolossova and Stroka, 2012; Rodrigues et al., 2019). The European Commission Regulation 1060/2013 approves the use of bentonite as a technical food additive, considering its belonging to four functional groups:

1. Substances that decrease the contamination of feed by mycotoxins. For this use, the Regulation allows bentonite identified as 1m558, which contains $\geq 70\%$ of smectite (di-octahedral montmorillonite), $< 10\%$ of opal and feldspar, and $< 4\%$ of quartz and calcite.
2. In order to make liquid food more homogenous and pelletize feed, bentonite is utilized as an addition.
3. anti-caking substances. In food that has been powdered, bentonite avoids lump formation.
4. contaminant-controlling agents for radionuclides.
5. The Regulation allows the use of 1 m558i bentonite, which contains less than 50% smectite, for the last three uses.

According to the same regulation, using mycotoxins as an adsorbent, binder, and anti-caking agent provides a maximum content of bentonite equal to 20,000 mg/kg of complete feed (with a moisture content of 12%). According to the FEEDAP Panel (2011), this is the maximum concentration with no side effects on the target species, the environment, or humans.

3. Materials and Methods

The administration of varying doses of bentonite in the absence of aflatoxins was tested on six lactating Friesian cows in a controlled experiment to determine any physiological responses, metabolic adaptations, and production changes in the cows. The experiment looked at a number of metabolites in rumen fluid. The University of Padua's OPBA (Organization in Charge of Animal Welfare) gave its approval to the experimental procedure (Prot. N. 0197903 of May 16, 2019; UOR: SI000139, Classif. III/13). This thesis work's focus is on a particular metabonomic analysis utilizing $^1\text{H-NMR}$ that was done on rumen fluid samples that were taken by esophageal tube from the animals used in the experiment and subsequently fermented in a lab under certain conditions (see later).

3.1. Animal recruitment and care

The "free stall" farm in Sant'Anna Morosina specifically purchased a healthy lactating primiparous Italian Friesian breed cow in order to execute the experimental test (PD). The mean standard deviation of the cows' lactation was 206 ± 23 days. At "Lucio Toniolo" experimental farm in Legnaro (PD), the animal was kept in individual boxes in a shed away from the other farm's cows. The cow had unlimited access to food while she was residing on the farm. All diets were distributed between 6:00 and 7:00 in the morning

in accordance with the NRC's (2001) recommendation for lactating cows with milk production of 35 kg/day. Table 1.1 displays the nutritional composition of the diets provided during the experiment on a DM basis. Two times a day, the cows were milked using the bucket method (at 6:00 and 17:00). This part of the experimental work was carried out in collaboration with the farm's personnel.

Table 1.1. Composition of the diet administered to the 6 cows during the entire experimental period.

| FOOD | %SS |
|------------------------------------------------------|-------|
| Medical | 1,35 |
| Corn Semolina | 1.53 |
| Protein Mix 36 (Northeast Agricultural Consortium) * | 3.06 |
| Multimix 5 (Northeast Agricultural Consortium) ** | 3.24 |
| Unilac Smc 500 Vitamin® (Nutristar) *** | 0.45 |
| Germolino® (Nutristar) **** | 0.36 |
| Dried Yeast | 0.045 |
| Corn silage | 4.8 |
| Grass silage | 4.5 |
| Molasses | 1.35 |

* *Complementary feed for dairy cows. Composition: hulled sunflower seed meal, roasted soybeans, feed based on hulled soybean meal, maize, sugar cane molasses.* ** *Complementary feed for ruminants. Composition: maize, barley, sugar cane molasses.* *** *Complementary mineral feed for lactating cows. Composition: calcium carbonate, sodium bicarbonate, sodium chloride, monocalcium phosphate, magnesium oxide, algal calcium (Lithotamnio), magnesium sulphate, monoammonium phosphate, dried seaweed *Ascophyllum nodosum* (TASCO) 1.8%, calcium sulphate dihydrate, wheat flour, potassium carbonate, sulfur flower, wheat.* **** *Complementary feed for dairy cows. Composition: expanded and blanched flax seeds, expanded and blanched maize germ, maize.*

3.2. Sample preparation for in vitro fermentation

Preparation of samples for the in vitro ruminal fermentation:

- 1) Ruminal fluid (RF) from one lactating cow collected by esophageal tube before feeding in the morning.
- 2) Medium Menke (MED)
- 3) RF + MED = Inoculum (IN)

Therefore, there are 14 samples:

- 2 × 25 mL of RF 1 + NaN₃ 5mM
- 2 × 25 mL of RF 2 + NaN₃ 5mM
- 2 × 25 mL of RF 3 + NaN₃ 5mM
- 2 × 25 mL of MED + NaN₃ 5mM
- 2 × 25 mL of IN 1 + NaN₃ 5mM
- 2 × 25 mL of IN 2 + NaN₃ 5mM

2 × 25 mL of IN 3 + NaN₃ 5mM

Experimental design:

| Rumen Fluid | Treatments | | | | | | Total |
|---------------------------------|---------------------|------------------------|-----------------------|------------------------|-------------------------|-------|-------|
| | B0 (0 mg bentonite) | B50 (2.5 mg bentonite) | B100 (5 mg bentonite) | B200 (10 mg bentonite) | B1000 (50 mg bentonite) | Blank | |
| 1 st esophageal tube | 5 | 5 | 5 | 5 | 5 | 2 | 17 |
| 2 nd esophageal tube | 5 | 5 | 5 | 5 | 5 | 2 | 17 |
| 3 rd esophageal tube | 5 | 5 | 5 | 5 | 5 | 2 | 17 |
| Total samples | 15 | 15 | 15 | 15 | 15 | 6 | 51 |

Pre-treatment of samples for NMR and ICP-OES.

There were two pre-treatments:

- Rotor JS 5.3: 7 × 4 positions = 28 positions

With one centrifugation, we can centrifuge all 14 samples in falcons (50 mL): This is done at 6800 × for 20 min at 4 °C. Then we transfer supernatants into a new falcon of 50 mL and filter with 0.22 µm syringe filters inside 2 falcons (15 mL). Finally, transfer aliquots into 3 cryopreservation (CP) tubes (2 mL).

- Rotor JA. 30. 50: 8 positions for 7 samples

We need only one centrifugation, but the samples must be transferred inside ultracentrifuge tubes (UC-tubes- 30 mL) before centrifugation. This is done at 17500 × g for 15 minutes at 4 °C. The next steps are like the previous ones.

At the end, store all the filtered samples at -80 °C.

Note: If the pre-treatment A was efficient, Rotor JS 5. 3 = 51 samples in 28 positions. In this case, each centrifugation takes 20 minutes. So, in total, we need two centrifugations. However, if pre-treatment A was not enough, step B followed. Rotor JA. 30. 50 = 51 samples in 8 positions. In this case, we need seven centrifugations, and each one takes 15 minutes.

After centrifugation, transferred supernatants are transferred to a Falcon (50 mL), filtered to 0.22 µm and collected inside the two Falcon (15 mL). Three aliquots are taken from the filtered samples and collected in CP-tubes. This part of the experimental work was carried out in collaboration with the Veterinary Physiology Lab of the Department of Comparative Biomedicine and Food Science (BCA).

At the end, we brought all the samples, which were prepared in Padova (Vallisneri) and stored at -80 °C.

3.2.1. In vitro procedure to study fermentation kinetics with ANKOM RF

The ANKOM RF was developed to study the in vitro kinetics of gas production that originated from microbial fermentative processes. The system is composed of fifty jars connected by means of a wireless data transmitter that sends the data to a computer. The computer records the pressure generated by the microbial fermentation's gas production. These pressure values are converted into gas volume (mL)

produced in a given period (min). This part of the experimental work was carried out in collaboration with the Department of Agronomy, Food, Natural resources, Animals and Environment (DAFNAE).

1) Reagents

- Menke Buffer

- demineralized water
- Sodium bicarbonate
- Ammonium bicarbonate
- Sodium biphosphate
- Monobasic potassium phosphate
- Magnesium sulfate heptahydrate
- Calcium chloride dihydrate
- Magnesium chloride tetrahydrate
- Cobalt chloride hexahydrate
- Iron chloride hexahydrate
- Resazurin (pH 6.9 indicator)
- H₂O
- Sodium hydroxide 1 M
- Sodium sulphate nonahydrate

2) ANKOM RF system

- 50 jars of 280 mL.
- ANKOM software
- Wireless GPM system, pressure detector.
- CO₂ introduction system in jars and air bleeding.

- Microbial inoculum

The best donors must not be pregnant or dry cows. The rumen fluid must be collected before feeding by 3 dry cows, feeding only with grass hay (ad libitum) and concentrate (2 kg/cow/day) (Table 1.2).

The animals must receive this diet for at least 15 days before the rumen fluid is collected.

Table 1.2. Feeding composition for dairy cows

| | % formula | NDF | Starch | PG |
|----------------------|-----------|------|--------|-------|
| Sunflower semi-décor | 15 | | | |
| Soy FE 44 | 20 | | | |
| Flour maize | 15 | | | |
| Flour barley | 20 | 29.5 | 26.85 | 12.76 |
| Dried beet pulps | 15 | | | |
| Grain bran | 15 | | | |

Ratio between substrate-microbial inoculum-medium

We use the ratio proposed by Menke (0.22g – 10 mL—20 mL):

Substrate 0.5 g; Microbial inoculum 25 mL: Medium 50 mL

Substrate 1.0 g; Microbial inoculum 50 mL: Medium 100 mL

A) Procedure to be conducted in the days before the incubation.

3) Medium preparation (Menke)

For the incubation of 50 jars content 0.05 grams of diet, are necessary 5 liters of medium (50 jars × 50 mL = 3 L di medium).

- Menke Buffer

The 4 solutions that compose the medium (buffer, macro-mineral, micro-mineral, and resazurin) could be prepared days before the incubation, while the reduction solution (solution B) must be prepared at the moment of use (the same day of the incubation). The day before the incubation, heat up the four solutions that compose the medium to a temperature of 39 °C. Then they will mix in the quantity and in the order indicated below.

solution A:

| | 1 L | 2 L | 6 L |
|------------------------------------|--------|-------|-------|
| Jars, n (1 g of diet per jar) | 9 | 18 | 45-55 |
| Demineralized H ₂ O, mL | 475.00 | 950.0 | 2850 |
| Micro-mineral solution, mL | 0.12 | 0.24 | 0.72 |
| Buffer solution, mL | 237.00 | 474.0 | 1422 |
| Macro-mineral solution | 237.00 | 474.0 | 1422 |
| Resazurin, mL | 1.22 | 2.44 | 7.32 |

Conserve the medium at the temperature of 39 °C until incubation.

- Substrate

The diet used as substrate previously was ground to a diameter of 1 mm and then weighted (0.5 ± 0.01 g). The substrate was put into the fermentation jars, which have not been enumerated yet (4 replications per substrate). Four jars must be incubated without substrate, like the white control. In our case, we weighted 1 g of diet (15 replies per thesis) and 6 white controls.

- Pre-incubation

After closing the jars with the pressure module measurement, they are put in the incubator at 39 °C (this is done to maintain the temperature in the system). It is essential that the jars be pre-heated at the time of adding the medium and the inoculum.

NB: Every temperature variation must determine a variation in the gas volume contained in the jars' headspace. This determines an alteration in the kinetics of gas production in the first phase of incubation.

B) Procedure to be carried out on the day of the incubation.

4) Incubation Procedure

- Medium

- Gurgel the CO₂ into the medium for at least 40 minutes.
- Keep on gurgling the CO₂ while adding the reduction solution until it turns. The solution turns first blue and then red. Until it becomes colorless (pH 6.9).
- Insufflate the CO₂ into the glass vase but not into the solution (the CO₂ in the liquid could alter the pH of the solution).

- Microbial inoculum

* Time of collection

The collection of the rumen fluid must be done in the morning before the distribution of the first feed (forage plus concentrate, or only concentrate if the animals have the forage *ad libitum*).

* Procedures to collect rumen fluid (at least three liters):

- Pre-heat the thermos with lukewarm water (40–45 °C).
- Insert the esophageal probe into the esophagus of the animal.
- Turn on the empty pump.
- Suck the rumen fluid across the esophageal probe into the collector container (1 liter of fluid).
- Turn off the empty pump.
- Remove the lukewarm water from the thermos and spill the rumen fluid in the thermos until it is full (filtering with three states of "dairyman gauze").
- Measure the temperature of the rumen fluid.
- Collect an aliquot of the rumen fluid to determine the pH.
- Collect an aliquot of the rumen fluid (8 mL) into a falcon with 2 mL of metaphosphoric acid to determine the N-NH₄.
- Bring the thermos to the laboratory as soon as possible (within 30 minutes of the collection).
- Collect the rumen fluids from 2-3 animals and then mix all the samples to obtain one global sample. This could be made in the laboratory, or on the farm (the important thing is the minimum contact between the rumen fluid and O₂).

* Conservation

The rumen fluid must be preserved in anaerobic conditions at a temperature of 39 °C. It is rash to insufflate CO₂, which could cool down the liquid. It is preferable to fill the thermos full (pay attention to the Campagne effect in the laboratory when the thermos is open!).

* Timing

The time that exists between the start of the collection and the start of the laboratory operations must be at least 1 hour, with specificity in the report.

* **Inoculum preparation**

After the medium's preparation, we continue with the addition of rumen fluid. During all the procedures of preparation, the CO₂ is gurgling in the container but not into the solution (modification of the medium's pH).

- **Incubation**

The solution is dosed with a dispenser in a quantity of 75 mL for every jar (50 medium + 25 inoculum = 75 mL). The operation must be realized in the minimum time possible (maximum 30 minutes) for the following reasons:

- i. Jars and molecules must not cool down (this could alter the gas measurements in the first phases of incubation).
- ii. The moment in which all the jars start the fermentation must be the same (if the time is different in the software, we can modify the time of the starting procedure for every jar).

The time of the incubator's stopping fermentation must be registered, just as the start of the process must be registered.

5) Procedure to be carried out at the end of incubation.

The operation depends on the aim of the study. Some could be:

- **Fermentation fluid:**

* **pH**

It is determined by the jars. It is useful to verify the efficiency and seal of the buffer system of the medium.

* **NH₃**

- i. Sample the supernatant; avoid shaking the jar's contents.
- ii. Put in the falcon 8 mL of the supernatant with 2 mL of metaphosphoric acid (solution in 25%).
- iii. Freezing since the moment to analyze (attention at the Champagne effect).

* **VFA**

- i. Sample the supernatant; avoid shaking the jar's contents.
- ii. Freezing 10 mL of supernatant since the moment to do the gas chromatography analysis.

- **Fermentation residual:**

If it is impossible to do the analysis immediately, the jars could be preserved in the fridge, at least for two days.

* **Dry matter and organic matter:**

- i. Empty the jars in the bask (the bask must be weighted with celite before use).
- ii. Dry in the heater for 12 hours.
- iii. Incubate at 550 °C for 3 hours.

* **NDF**

- i. Empty the jars into the Ankom F57 bags.
- ii. Determine NDF with the Ankom method.

iii. Incinerate at 550 °C for the data and AIA's correction.

*** Nitrogen balance**

The following procedures plan the interruption of the fermentation process in the moment in which there is:

I. The maximum production of gas or

II. The production of the other half of the total gas production ($t^{1/2}$).

Getachew et al. (2001) and Gring et al. (2005):

Microbial N = "feed N" – "N-NDF" – " Δ N-NH₃"

"NDF-N" = nitrogen link to NDF, that is available at the end of the fermentation

" Δ N-NH₃" = variation of the ammoniacal nitrogen level at the end of the incubation.

Solution that made Menke medium

A. Buffer Solution (Maximum duration 1 month)

| | g/L | g/1.5 L | g/2 L |
|----------------------------------------------|------|---------|-------|
| Jars, n (1 g of diet per jar) | 9 | 18 | 45-55 |
| NaHCO ₃ , g | 35.0 | 52.5 | 70.0 |
| (NH ₄) HCO ₃ , g | 4.0 | 6.0 | 8.0 |
| Make up the solution with distilled water, L | 1 | 1.5 | 2 |

B. Macro-mineral solution (Maximum duration 1 month)

| | g/L | g/1.5 L | g/2 L |
|----------------------------------------------|-----|---------|-------|
| Jars, n (1 g of diet per jar) | 9 | 18 | 45-55 |
| Na ₂ HPO ₄ , g | 5.7 | 8.55 | 11.4 |
| KH ₂ PO ₄ , g | 6.2 | 9.3 | 12.4 |
| MgSO ₄ ×7H ₂ O | 0.6 | 0.9 | 1.2 |
| Make up the solution with distilled water, L | 1 | 1.5 | 2 |

C. Micro-mineral solution (Maximum duration 6 months)

| | g/100 mL |
|---------------------------------------------------------------------------------------------|----------|
| CaCl ₂ ×2 H ₂ O, g | 13.2 |
| MnCl ₂ ×4 H ₂ O, g | 10.0 |
| CoCl ₂ ×6 H ₂ O, g | 1.0 |
| FeCl ₃ ×4 H ₂ O, g (FeCl ₃ ×6 H ₂ O, g = 0.8 g) | 0.57 |
| Make up the solution with distilled water, L | 100 |

D. Resazurin solution (maximum duration 6 months)

| | g/100 mL |
|----------------------------------------------|----------|
| Resazurin, g | 0.1 |
| Make up the solution with distilled water, L | 100 |

E. Reduction solution (solution B)

The preparation must be done at the moment of use in the ultrasound bath or at 40 °C.

| | g/L of A Sol. | g/2 L of A Sol. | g/6 L of A Sol. |
|------------------------------------------------------------------------------------------|---------------|-----------------|-----------------|
| Jars, n | 9 | 18 | 45-55 |
| NaOH 1M, (40 g NaOH in 1 L of water), mL | 2.0 | 4.0 | 6.0 |
| Na ₂ S×9 H ₂ O, mg (Na ₂ S×7 H ₂ O = 285 mg) | 336.0 | 672.0 | 2016.0 |
| Distilled water, mL | 47.5 | 95.0 | 285.0 |

3.3. ¹H-NMR spectroscopy of rumen fluid

The samples of rumen fluid were examined using ¹H-NMR analysis in the Department of Molecular Medicine at the University of Padua.

3.3.1. Preparation of rumen fluid samples

To optimize the procedure to be used for the sample preparation for ¹H-NMR spectroscopy, a literature search was conducted. However, only a few metabonomic studies employing ¹H-NMR on rumen fluid and various techniques have been found (Ametaj et al., 2010; Bica et al., 2020; O'Callaghan et al., 2018; Saleem et al., 2013, 2012; Zhao et al., 2014). Extensive work was then conducted in the laboratory to fine-tune the following sample preparation procedure:

- 1) Rumen fluid aliquots are melted at room temperature.
- 2) Centrifugation at 17530 g for 30 minutes at 22 °C
- 3) Filtration with 0.22 µm syringe filters
- 4) recording of the filtrate's pH in its current state

The sample preparation for ¹H-NMR spectroscopy was carried out by the consecutive steps described below:

- i. 5 mM NaN₃ was added to 180 µL of potassium phosphate (K/Pi) 1.5 M buffer at pH 7.4.
- ii. 70 µL of a 40 mM solution of Trimethyl Silyl Propionic Acid (TSP) in heavy water (D₂O).
- iii. 450 µL of filtered rumen fluid (700 µL is thus obtained as the total sample volume).
- iv. measurement of the pH of the ¹H-NMR sample just before the spectrum is acquired.
- v. 600 µL of the final solution are transferred into an NMR tube (Wilmad 535-PP, diameter 5 mm).
- vi. To reduce interference from external materials, the tubes were degreased with acetone before being placed in the magnet.

The addition of the buffer is beneficial for pH control, which is essential in NMR spectroscopy. It is known that even slight changes in pH cause some peaks of the NMR spectrum to shift in position in proportion to the change itself, as well as affect the line shape of the peaks themselves. Working in a pH range between 7.25 and 7.35 (with an average value of 7.30 ± 0.4) was made possible by the addition of the buffer. The TSP is utilized as an internal reference for the 0-ppm signal. D₂O at 10% in the sample, on

the other hand, keeps the resonance frequency and magnetic field connected (lock to deuterium) in the face of any micro-variations or thermal drifts of the latter.

3.3.2. Acquisition of NMR spectra

The Larmor frequency for ^1H , which, at a magnetic field (B_0) value of 7 Tesla, is 300.13 MHz, was used to acquire all of the ^1H -NMR spectra, and the working temperature was adjusted at 300 K with a stabilization of roughly 0.1 K. For each sample's temperature to settle, 5 minutes have always been allowed to pass from the insertion of the sample before acquiring the spectrum. Similarly to pH variations, even minimal temperature variations induce position shifts of the peaks of the NMR 1D spectrum.

Four separate one-dimensional spectra were acquired for each rumen fluid sample using four different pulse sequences:

- Zgpr sequence: It optimizes the suppression of the water signal, which would otherwise overwhelm that of other molecules due to its size and intensity. This sequence is utilized to determine the ideal water suppression settings that will be enforced throughout the succeeding acquisition sequences.
- The NOESY sequence is the classical method for acquiring an NMR 1D spectrum. It involves emitting a 90-degree radio frequency pulse, followed by the acquisition of the signal that is emitted, and it is optimized by superimposing a magnetic field gradient along the Z axis. Since no digital filters are applied during this acquisition process, it is typically employed for the quantitative measurement of the amounts of nuclear species found in the NMR spectrum.
- The CPMG sequence (Carr-Purcell-Meiboom-Gill) makes use of a digital filter to minimize the wide-spectrum signals produced by macromolecules (for instance, proteins and lipids) in the samples, thus allowing for better identification of low-molecular-weight species (metabolites). In the field of metabolomic research, it is the sequence that is most frequently employed for qualitatively assessing the signals in an NMR spectrum. For each sample, the CPMG sequence was used to acquire two spectra, the first with 64 scans to quickly verify the quality of the spectrum and the second with 512 scans to increase the signal-to-noise ratio and better define the peak profile (for the other sequences, only one spectrum per sample was acquired with 64 scans).
- The DOSY sequence employs a digital filter that serves the opposite purpose from that of the CPMG sequence. It filters and minimizes the signals caused by small molecules, allowing for a better evaluation of the signals caused by macromolecules, which are typically present in an NMR spectrum as broad bands underneath the narrow peaks of small molecules.

All spectra, regardless of the type of scan, were acquired with a time domain (TD, number of points collected in the time space) of 64K points of FID, a spectral width (SW, sweep width) of 30 ppm (corresponding to 9014 Hz), 4 dummy scans, an acquisition time (AQ) of 3.635 s, and a relaxation time

(RD) of 4 seconds. The spectra were processed using a multiplicative Lorentzian function with a 0.3 Hz line width before the Fourier transform was applied.

The Bruker TopSpin version 3.5 software was used for both the acquisition and processing of the spectra. By setting the peak of the TSP standard to 0 ppm, the position of the peaks on the spectral scale was internally calibrated.

3.3.3. Qualitative analysis of $^1\text{H-NMR}$ spectra

The $^1\text{H-NMR}$ spectra were subjected to metabolomic analysis in order to look for signals associated with the metabolites present in the rumen fluid. Three of the aforementioned studies (Ametaj et al., 2010, Saleem et al., 2012, and Zhao et al., 2014) were reviewed to cross-check the identified metabolites, as well as various databases for the same purpose (Chemical Book, BMDB, and HMDB), on the basis of the type of signal (singlet (s), doublet (d), triplet (t), quartet (q), or multiplet (m)) and the location of each peak on the spectrum.

A further step was made for some metabolites: by superimposition, the corresponding pure standards were purchased, and the presence of the metabolite in the samples' spectra was identified by superimposition with the spectra obtained from the standards under the same conditions as the samples (Figure 1.24).

During the study, there were signals that caught our attention. The spectrum acquired from the syringe filters' cleaning solution, which was collected from the same package as those used to prepare the rumen fluid samples, revealed the presence of some peaks also present in the sample's spectra. This cleaning liquid was created by filtering water through MilliQ, and its spectrum was taken under the same operating conditions as the samples. Such a procedure allowed us to identify some contaminants, such as glycerol, and exclude their signals from the following qualitative and statistical analysis.

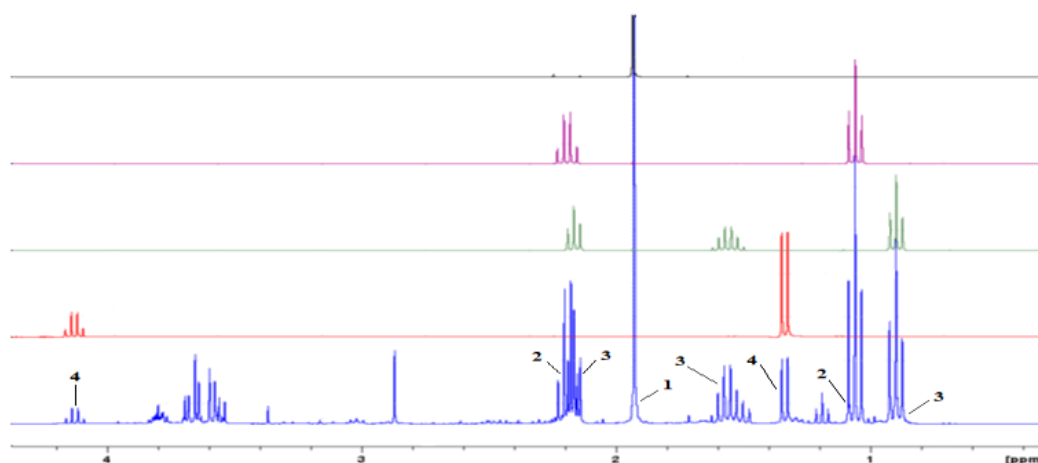


Figure 1.24. Identification of the spectral signals relating to the metabolites studied on the $^1\text{H-NMR}$ spectrum of one of the rumen liquid samples (blue) and comparison with the spectra obtained from the single standards. Numeric code: 1: Acetate; 2: Propionate; 3: Butyrate; 4: Lactate. Color code: Blue: rumen fluid; Red: Na-Lactate; Green: Na-Butyrate; Purple: Na-Propionate; Black: Na-Acetate

3.3.4 Evaluation of mineral and heavy metals content

Two 1.5-mL aliquots of each treatment group were frozen at room temperature and centrifuged at 17000 g for five minutes at room temperature in order to determine the metal content by ICP-OES. 1 mL of each supernatant was brought to a final volume of 4 mL by the addition of a 5% nitric acid solution. This oxidizing solution was allowed to incubate for a whole night at room temperature. Then, the concentration of Al, As, Ba, Ca, Cd, Co, Cr, Cu, Fe, K, Li, Mg, Mn, Mo, Na, Ni, P, Pb, Se, Sr, and Zn was measured using an ICP-OES 5110 (Agilent) spectrometer that operates with argon plasma. Six standard solutions at various concentrations (0.010, 0.020, 0.050, 0.100, 0.200 ppm for Fe, Ca, and Mg; 0.050, 0.100, 0.500, 1.000, 2.000 ppm for K; 0, 0.300, 0.600, 1.000, 3.000, 6.000 ppm for Na and P; 0.005, 0.010, 0.050, 0.100, 0.200 ppm for the other elements) were prepared using certified single-element standards from Agilent for the calibration curves. The samples were further diluted 1:300 (v/v) with a 5% aqueous solution of HNO₃ in order to measure the elements present in higher concentrations (Ca, K, Mg, Na, and P).

3.4. Data analysis and statistical processing

The data analysis performed on the ¹H-NMR spectra followed the steps illustrated in Figure 1.29 Starting with the individual marker metabolites, the statistical analysis uses univariate statistics to assess any alterations in these metabolites brought on by bentonite treatment. Then continues by extending the investigation using multivariate statistical analysis to include the entire ruminal metabolome (PCA).

3.4.1. Multivariate Statistical Analysis: Principal Component Analysis (PCA)

The statistical approach most commonly used in metabonomics is not limited to evaluating the concentration of single metabolites alone. Instead, it produces graphs in which one can observe if the points representing the spectra are clustered or not—if present, any cluster consists of spectra similar but different from those of another cluster. Belonging to one group rather than another depends on many independent variables, which is why multivariate statistics are used.

This thesis uses the multivariate statistical analysis technique of PCA (*Principal Components Analysis*). The entire NMR spectrum of each sample examined is divided into several intervals called "buckets" that can be (as they generally are) of the same spectral width; each bucket contains a spectral portion, the area of which is calculated. Such calculated values generate the so-called "Bucket Table". A single NMR spectrum is thus represented by a set of buckets in each table row, making the full bucket table the numerical representation of all the NMR spectra in question as "areas of spectral intervals".

This numerical table serves as the input data for the PCA, whose goal is to understand how the metabolic profiles (understood as a multifactorial unicum) vary from one spectrum to another (in this case, a spectrum is representative of a given bovine subjected to a given treatment). The variance of every bucket

(i.e., every column) is calculated for the entire bucket table, and consequently, the variances of the concentrations of the various metabolites are used as new variables.

In summary, the data (or variables) that make up the bucket table insist in the spectroscopic space, which has coordinates $x = \text{frequency range (ppm)}$ (= width of the bucket) and $y = \text{spectral intensity}$. To work with the PCA analysis, we pass from the spectroscopic space to another space whose variables are no longer the buckets' values but become the values of the variance's Principal Components (PC). More specifically, we move from the 2D spectroscopic space to a multidimensional space, whose variables are no longer the original values of the buckets but rather the values of the PC. For the graphic interpretation of the results, the multidimensional space is divided into several two-dimensional spaces, 2D, obtained by considering a different pair of principal components each time. For example, PC1 vs. PC2 is the 2D space in which the axes are PC1 and PC2. The variables are represented by the values of the main components, PC1 and PC2.

To achieve this, two tables known as the "Scores Table" and the "Loadings Table" are constructed starting from the scores and loading values calculated by the PCA analysis. In the table of scores, each row contains the total variance of a single spectrum. The total variance of a single spectrum is represented by the entire set of the various Principal Components (PC1, PC2,..., PCn), calculated along the entire bucket table, whose individual values are contained in the cells of the row. Thus, each spectrum is divided into as many cells as there are PC_i (PC1, PC2, PC3, etc.) of the variance. Each PC_i has a different statistical weight in the "explanation" of the total variance, and the various PC_i are sorted along the table row in descending order of statistical weight (PC1 > PC2 > PC3).

On the other hand, in the loadings table, each column corresponds to a single Principal Component (PC_i), and each row corresponds to a specific bucket. The cells of this table contain the loadings of all the PC_i: each column contains the "total loading" of a specific PC_i, and each cell of a column contains the contribution of a specific bucket to that PC_i. Thus, considering the rows of the loading table, each of them contains the contribution of a specific bucket to the loadings of all the PC_i, with each cell containing the contribution of that bucket to the loadings of the various single PC_i.

For a better understanding of the phenomenon underlying the numbers, these types of numerical tables must be "translated" into two-dimensional graphical representations, specifically into graphs known as SCORES PLOT and LOADINGS PLOT (Figure 1.25).

The points reported in the SCORES PLOT (i.e., the scores), one for each sample (i.e., one point for each spectrum), have as coordinates the various PC_i; therefore, we obtain as many plots as possible, two-by-two combinations of the various PC_i. For example, in the plot where PC1 vs. PC2 is graphed, each spectrum is represented by a point having as coordinates the values of PC1 and PC2 of that spectrum. In conclusion, choosing to represent a spectrum in a PC1 vs. PC2 graph means placing a point (the spectrum) graphically at the coordinate position (PC1, PC2); choosing to represent the same spectrum in a PC3 vs. PC5 graph means going to place it at a coordinate position (PC3, PC5), and so on.

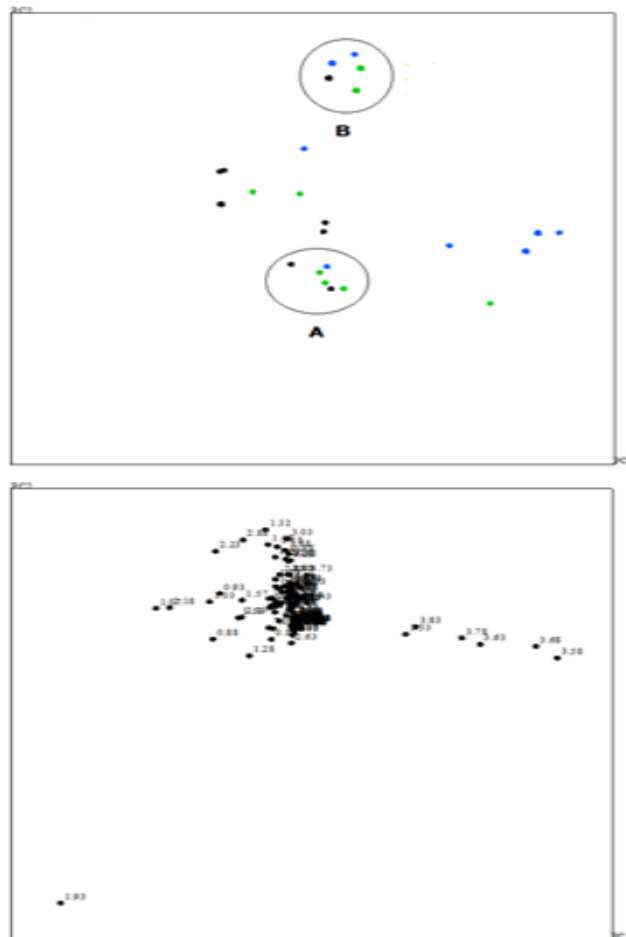


Figure 1.25. Example of scores plot (top) and loadings plot (bottom). In particular, the scores of cluster A are spectra similar to each other but different from the spectra of cluster B.

The points on the graph may eventually group together; if this occurs, each grouping represents a collection of spectra that are similar to one another, while the outlier points represent spectra that are different from the rest for a certain statistical variable.

To better use the graphs, the operator provides a color to the scores depending on whether the reference sample is a member of a group in order to create a clearer visual representation of any eventual groupings (in this thesis, it means coloring, for example, based on belonging to a treatment group). The values of the so-called loadings, which are depicted in the LOADINGS PLOTS, determine the relationship between the points of the Scores Plots and the original spectroscopic space (i.e., the areas underlying the spectroscopic peak). In the Loadings Plot each bucket is represented by a point that is situated in a position of coordinates that matches the statistical weights that each bucket contributes to the specific PCi.

For a visual interpretation of the PCA analysis' results, the scores and loadings plots must be observed together: buckets grouped in the loadings graph have little weight in determining the differences or trends found in the corresponding score plot (i.e., variance), while buckets far from the groupings are more responsible for the differences between the points of the corresponding plot of the scores. Therefore, they are more responsible for the statistical differences between the groups of spectra.

The ^1H -NMR spectra included in this thesis were subjected to multivariate statistical analysis using the AMIX (Bruker) software version 3.9.11. Analysis was done without considering the region between 4,530 and 5,100 ppm that corresponds to the water signal (to avoid the artifacts introduced by the pulse sequences for the pre-saturation of the water).

4. Result and discussion

According to the European Union (2021), the clay mineral bentonite, a member of the phyllosilicate family, is used as an animal feed additive. In fact, clay minerals have generally positive impacts on animal physiology because they serve as binders to create pelleted feed and as adsorbents for mycotoxins and heavy metals (Ghadiri et al., 2015; Nadziakiewicz et al., 2019; Slamova et al., 2011). However, other investigations noted potential negative outcomes from clay treatment both *in vitro* and *in vivo*, including mineral and vitamin imbalances, interactions with veterinary medications, intestinal toxicity, liver damage, and reduced growth performance (Elliott et al., 2019). Due to their potential impact on the intestinal and/or ruminal microbiota, which could affect fermentative processes and metabolite availability, clay minerals can interact with microorganisms (Cuadros, 2017); therefore, their administration could become relevant for animal physiology.

This thesis is a preliminary investigation of the potential impacts of zootechnical bentonite on the rumen metabolome. Rumen fluid samples to be utilized for metabolomic investigations and metabonomics were obtained using esophageal tube in order to prevent chemical and microbial contamination of the upper alimentary canal as well as to guarantee the most accurate determination of rumen pH (Duffield et al., 2004; Garrett et al., 1999). In accordance with the relevant lectures (Eom et al., 2021; Wang et al., 2021), it was decided to conduct these studies using ^1H -NMR spectroscopy because this technique enables not only the observation of the whole metabolic profile of each rumen fluid sample but also the identification and quantification of the specific metabolites present in it.

4.1 Results of metabolomic analysis by ^1H -NMR

The spectra obtained with the 512-scan CPMG sequence allowed for the best identification of low-molecular-weight species when the spectral signals associated with rumen metabolites were identified. The metabolites in this thesis work were identified by comparing the multiplicity and positions of the peaks with the data reported in the databases available in the literature (Bovine Metabolome Database, BMDB, and Human Metabolome Database, HMDB), as well as by adding known concentrations of the single pure metabolites (Sigma-Aldrich) to the samples. This was done by a two-step procedure consisting firstly of a superimposition of the spectra of the pure metabolite's standard to the sample spectra and secondly of the addition of a pure standard solution to the samples and repeating the acquisition of the NMR spectra (in this way, the peaks of the specifically searched metabolites increase due to the addition of the standard). The spectral analysis allowed us to identify 24 metabolites (Acetate,

Acetylcarnitine, Alanine, Butyrate, Carnitine, Dimethylamine, Ethanol, Formate, Galactose, Glucose, Histidine, Isoleucine, Isovalerate, Leucine, Methylamine, Oxoglutarate, Phenylalanine, Propionate, Sarcosine, Succinate, Trimethylamine, Tryptophane, Tyrosine, and Valine) whose positions in the spectrum are reported in Figure 1.26.

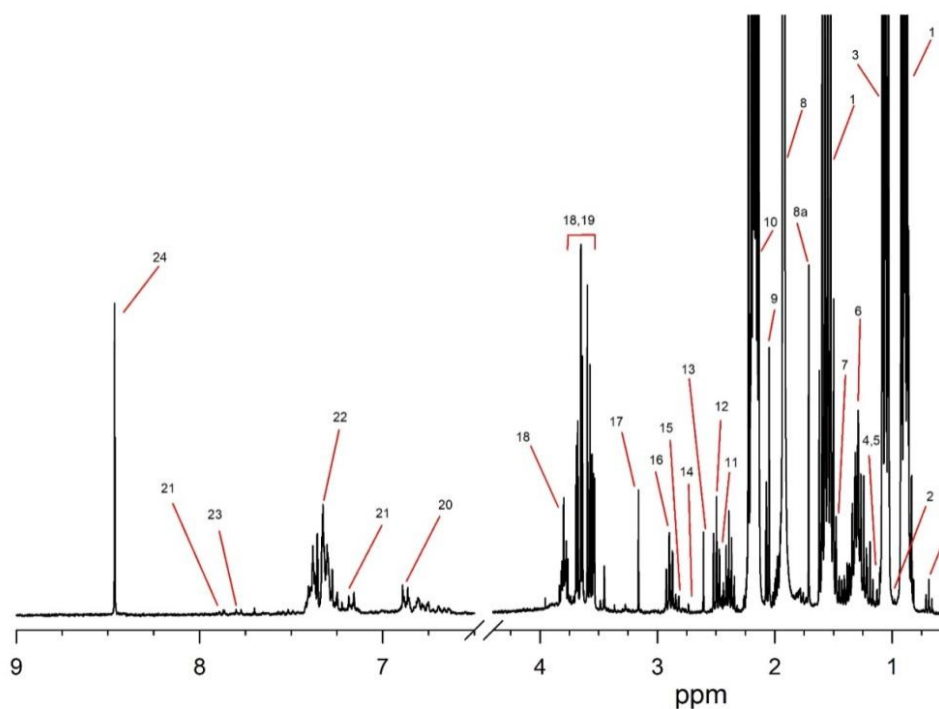


Figure 1.26. Typical ^1H -NMR spectrum obtained from Rumen Fluid samples. 1. Butyrate, 2. Valine, 3. Propionate, 4. Leucine, 5. Isoleucine, 6. Ethanol, 7. Alanine, 8. Acetate, 8a. Acetate satellite, 9. Isovalerate, 10. Acetylcarnitine, 11. Succinate, 12. Dimethylamine, 13. Methylamine, 14. Sarcosine, 15. Trimethylamine, 16. Oxoglutarate, 17. Carnitine, 18. Glucose, 19. Galactose, 20. Tyrosine, 21. Histidine, 22. Phenylalanine, 23. Tryptophane, 24. Formate

Using the same spectrum, the metabolite concentrations were measured. This option is made possible by the fact that the ^1H -NMR spectra were recorded using the same acquisition parameters, so any artifacts caused by the digital filter of the CPMG sequence are present in all spectra, including that of the external standard: The weight of this digital filter is effectively cancelled because the concentration is measured as a measurement normalized to the concentration of an external standard. This allows for the quantification of the metabolites on CPMG sequence-derived spectra rather than the common NOESY-derived spectra. To highlight any variations in the metabolic profile caused by bentonite, the collected ^1H NMR spectra were processed for the study of the main components of variance (PCA). The analysis was done with the help of the AMIX 4.0.1 program (Bruker Biospin), applied to the spectral range of 0.5–10.0 ppm, and separated into regular rectangular intervals (buckets) of 0.05 ppm. Excluded from the analysis was the spectral range containing the signals of pollutants and water. Despite the small number of samples and replicates, the PCA results show a clear trend to distinguish the metabolic profile with bentonite dosage. Because the high fluctuation of abundant metabolites hides group differences in low-abundance

metabolites, the original variable values were normalized to the total intensity of the spectra and then subjected to Pareto scaling to lessen the masking impact of the more intense variables on the less intense ones. Yang et al. (2015) demonstrated that scaling with the Pareto mathematical procedure (User's Guide to SIMCA-P, 2005) reduces magnitude masking without increasing measurement deviation. As a result, they showed that by deleting missing values and decreasing the mask effect, the devised preprocessing approach could enhance the analysis of a multivariate data set of metabolomics.

The PCA analysis demonstrated a distinct separation between the sample without bentonite and the samples added with bentonite, with PC1 and PC2 explaining 83.92% of the total variance (69.59% and 14.33%, respectively). These analyses also identified the spectral ranges that include the signals of butyrate and propionate as being responsible for such a variance, giving the indication of a decreasing concentration of butyrate and an increasing concentration of propionate for the samples added with bentonite (Figure 1.32).

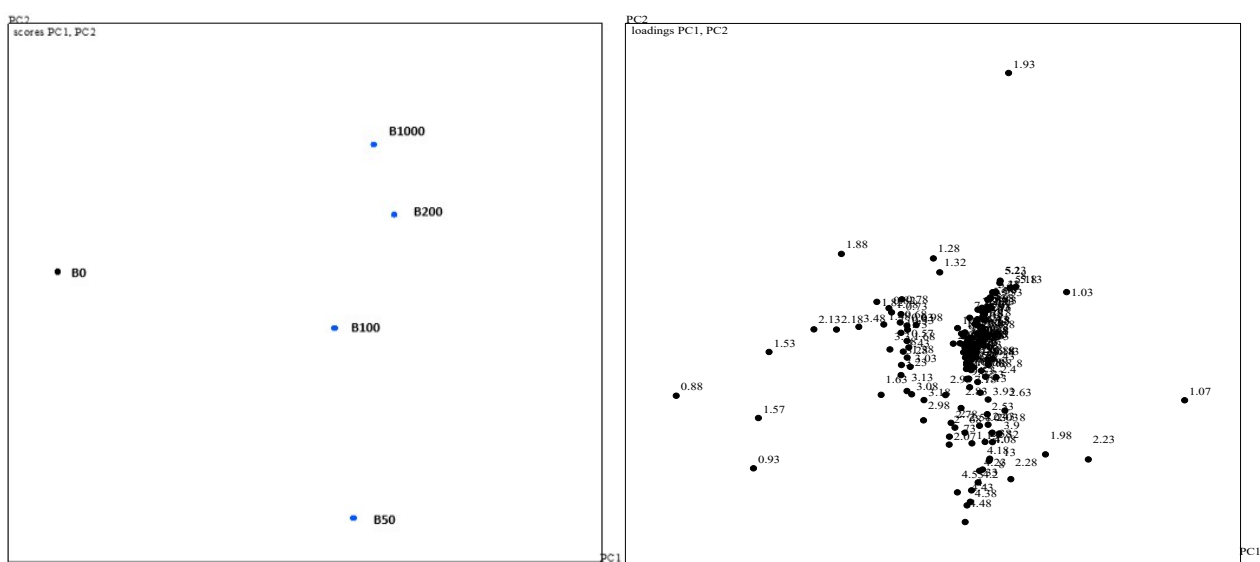


Figure 1.27. Scores plot (left) and loadings plot (right) of the two first principal components (PC1 and PC2) of the PCA analysis: Each point in the Scores plot represents a sample, in the loadings plot represents a spectral region.

4.2. Results of the mineral and heavy metal content by ICP-OES

The measured concentrations of Ba, Co, Cr, Cu, Mo, and Se were in the nanomolar range. The macrominerals, including Ca, K, Mg, Na, and P, were instead in the millimolar range, while Al, Fe, Li, Mn, and Sr were in the micromolar range. As, Cd, and Pb values were not taken into consideration because their concentrations were below the detection threshold. The zinc concentration was considered unreliable since it was subjected to a noticeable matrix effect. A regression analysis using SPSS software was conducted to determine whether there was any correlation between bentonite additions and mineral concentrations. The results showed that as bentonite dosages increased, Ba, Ca, and Mn concentrations significantly decreased, while Al, Cr, Mo, and Sr concentrations significantly increased (Table 3.4). The concentrations of the other examined components did not significantly change.

Table 1.3. Regression analysis between the dose of bentonite and mineral concentrations. Only minerals that showed a significant Standardized Regression Coefficient (Beta) with increasing dosage of bentonite are reported.

| Minerals | Fitting | Beta | Beta ² | F | B0 (μM) | B1 |
|----------|-------------|--------|-------------------|-----------|------------------|--------------------------|
| Al | Linear | 0.894 | 0.799 | 11.951* | 1.610 ± 0.058 | 4000 × 10 ⁻⁴ |
| Ba | Exponential | -0.964 | 0.900 | 38.992** | 0.197 ± 0.008 | -0.001 |
| Ca | Exponential | -0.895 | 0.802 | 12.139* | 982.730 ± 85.699 | -0.001 |
| Cr | Linear | 0.958 | 0.917 | 33.246** | 0.216 ± 0.001 | 1.781 × 10 ⁻⁵ |
| Mn | Exponential | -0.945 | 0.893 | 25.163* | 6.262 ± 0.303 | -0.001 |
| Mo | Linear | 0.906 | 0.821 | 13.771* | 0.048 ± 0.004 | 3.316 × 10 ⁻³ |
| Sr | Linear | 0.987 | 0.975 | 115.523** | 1.317 ± 0.030 | 0.001 |

Linear model: $Y = b_0 + b_1 \cdot X$; Exponential model: $Y = b_0 \cdot e^{(b_1 \cdot X)}$; * $P < 0.05$; ** $P < 0.01$.

5. Conclusion

The purpose of this preliminary investigation was to determine the suitability of using ¹H NMR and ICP-OES techniques to explore the rumen fluid metabolome in dairy cows. The results, particularly those related to the effect of bentonite administration, revealed the accuracy of both spectroscopic approaches in analyzing alterations in the rumen fluid metabolome. Despite the small number of samples and repetitions, the utility of ¹H NMR and ICP-OES spectroscopy for analyzing the rumen fluid metabolome and mineral contents was confirmed.

6. Acknowledgment

I am sincerely grateful and deeply thankful to all the individuals who supported me during my two-year study at the University of Padova. First and foremost, I would like to express my wholehearted gratitude to my family, including my father, mother, and two brothers, who provided me with the opportunity to come to Italy and supported me throughout my journey. Their unwavering support and encouragement have played a significant role in my accomplishments.

I would also like to extend my heartfelt thanks to my fiancé, Parimah, who has been a constant source of love and support. Despite the challenges of being far apart, your presence and kindness have meant the world to me, and I deeply appreciate your unwavering support.

I am immensely grateful to my supervisor, Prof. Fabio Vianello, and my advisors, Prof. Lucio Zennaro and Prof. Gianfranco Gabai. Their guidance and assistance throughout my thesis have been invaluable, expanding my knowledge and perspective as a Master's student. In particular, I would like to express my gratitude to Prof. Zennaro and Dr. Anna Damato, with whom I have spent a significant amount of time in the NMR lab. Their influence and mentorship will forever remain in my heart. Each of you has had a meaningful impact on me and has provided a platform for personal and intellectual growth.

Once again, I want to express my deepest gratitude to all those who have played a part in my journey. Your support, love, and guidance have shaped my experiences and contributed to my personal and academic growth.

7. Reference

- Adamis, Z., R. B. Williams, and J. Fodor. 2005. Bentonite, kaolin, and selected clay minerals. No. 231. World health organization.
- Akin, D. and W. Borneman. 1990. Role of rumen fungi in fiber degradation. *Journal of Dairy Science* 73(10):3023-3032.
- Al-Ani, T. and O. Sarapää. 2008. Clay and clay mineralogy. Physical-chemical properties and industrial uses.
- Alonso, A., M. A. Rodríguez, M. Vinaixa, R. I. Tortosa, X. Correig, A. Julià, and S. Marsal. 2014. Focus: a robust workflow for one-dimensional NMR spectral analysis. *Analytical chemistry* 86(2):1160-1169.
- Ametaj, B. N., Q. Zebeli, F. Saleem, N. Psychogios, M. J. Lewis, S. M. Dunn, J. Xia, and D. S. Wishart. 2010. Metabolomics reveals unhealthy alterations in rumen metabolism with increased proportion of cereal grain in the diet of dairy cows. *Metabolomics* 6:583-594.
- Barrientos-Velázquez, A. L., S. Arteaga, J. B. Dixon, and Y. Deng. 2016. The effects of pH, pepsin, exchange cation, and vitamins on aflatoxin adsorption on smectite in simulated gastric fluids. *Applied Clay Science* 120:17-23.
- Barton, C. and A. Karathanasis. 2002. Clay minerals. Vol. 10. Marcel Dekker: New York.
- Benincasa, C., J. Lewis, G. Sindona, and A. Tagarelli. 2008. The use of multi element profiling to differentiate between cow and buffalo milk. *Food chemistry* 110(1):257-262.
- Bica, R., J. Palarea-Albaladejo, W. Kew, D. Uhrin, D. Pacheco, A. Macrae, and R. J. Dewhurst. 2020. Nuclear magnetic resonance to detect rumen metabolites associated with enteric methane emissions from beef cattle. *Scientific Reports* 10(1):5578.
- Boss, C. B. and K. J. Fredeen. 2004. Concepts, instrumentation and techniques in inductively coupled plasma atomic emission spectrometry. Perkin-Elmer, Incorporated
- Brandao, G. C., G. D. Matos, and S. L. Ferreira. 2011. Slurry sampling and high-resolution continuum source flame atomic absorption spectrometry using secondary lines for the determination of Ca and Mg in dairy products. *Microchemical Journal* 98(2):231-233.
- Braun, U., T. Rihs, and U. Schefer. 1992. Ruminal lactic acidosis in sheep and goats. *The Veterinary Record* 130(16):343-349.
- Bremer, J. 1983. Carnitine--metabolism and functions. *Physiological reviews* 63(4):1420-1480.
- Chen, L., X. Li, Z. Li, and L. Deng. 2020. Analysis of 17 elements in cow, goat, buffalo, yak, and camel milk by inductively coupled plasma mass spectrometry (ICP-MS). *RSC advances* 10(12):6736-6742.
- Danielsson, R., J. Dicksved, L. Sun, H. Gonda, B. Müller, A. Schnürer, and J. Bertilsson. 2017. Methane production in dairy cows correlates with rumen methanogenic and bacterial community structure. *Frontiers in microbiology* 8:226.

- Di Gregorio, M. C., D. V. d. Neeff, A. V. Jager, C. H. Corassin, Á. C. d. P. Carão, R. d. Albuquerque, A. C. d. Azevedo, and C. A. F. Oliveira. 2014. Mineral adsorbents for prevention of mycotoxins in animal feeds. *Toxin Reviews* 33(3):125-135.
- Eom, J. S., E. T. Kim, H. S. Kim, Y. Y. Choi, S. J. Lee, S. S. Lee, S. H. Kim, and S. S. Lee. 2021. Metabolomics comparison of rumen fluid and milk in dairy cattle using proton nuclear magnetic resonance spectroscopy. *Animal Bioscience* 34(2):213.
- Garrett, E., M. Pereira, K. Nordlund, L. Armentano, W. Goodger, and G. Oetzel. 1999. Diagnostic methods for the detection of subacute ruminal acidosis in dairy cows. *Journal of dairy science* 82(6):1170-1178.
- Goldansaz, S. A., A. C. Guo, T. Sajed, M. A. Steele, G. S. Plastow, and D. S. Wishart. 2017. Livestock metabolomics and the livestock metabolome: A systematic review. *PloS one* 12(5):e0177675.
- Güler, Z. 2007. Levels of 24 minerals in local goat milk, its strained yoghurt and salted yoghurt (tuzlu yoğurt). *Small Ruminant Research* 71(1-3):130-137.
- Harfoot, C. 1981. Lipid metabolism in the rumen. *Lipid metabolism in ruminant animals*:21-55.
- Hogarth, C. J., J. L. Fitzpatrick, A. M. Nolan, F. J. Young, A. Pitt, and P. D. Eckersall. 2004. Differential protein composition of bovine whey: a comparison of whey from healthy animals and from those with clinical mastitis. *Proteomics* 4(7):2094-2100.
- Hoover, W. H. and T. K. Miller. 1991. Rumen digestive physiology and microbial ecology. *Veterinary Clinics of North America: Food Animal Practice* 7(2):311-325.
- Klein, M. S., M. F. Almstetter, G. Schlamberger, N. Nürnberger, K. Dettmer, P. J. Oefner, H. Meyer, S. Wiedemann, and W. Gronwald. 2010. Nuclear magnetic resonance and mass spectrometry-based milk metabolomics in dairy cows during early and late lactation. *Journal of dairy science* 93(4):1539-1550.
- Kolossova, A. and J. Stroka. 2012. Evaluation of the effect of mycotoxin binders in animal feed on the analytical performance of standardised methods for the determination of mycotoxins in feed. *Food Additives & Contaminants: Part A* 29(12):1959-1971.
- Lachenmeier, D. W., E. Humpfer, F. Fang, B. Schutz, P. Dvortsak, C. Sproll, and M. Spraul. 2009. NMR-spectroscopy for nontargeted screening and simultaneous quantification of health-relevant compounds in foods: the example of melamine. *Journal of agricultural and food chemistry* 57(16):7194-7199.
- Lou, J., K. Dawson, and H. Strobel. 1997. Glycogen formation by the ruminal bacterium *Prevotella ruminicola*. *Applied and Environmental Microbiology* 63(4):1483-1488.
- Mazzei, P. and A. Piccolo. 2012. ¹H HRMAS-NMR metabolomic to assess quality and traceability of mozzarella cheese from Campania buffalo milk. *Food Chemistry* 132(3):1620-1627.
- Nadziakiewicz, M., S. Kehoe, and P. Micek. 2019. Physico-chemical properties of clay minerals and their use as a health promoting feed additive. *Animals* 9(10):714.

- Nickel, R., A. Schummer, and E. Seiferle. 1979. Trattato di anatomia degli animali domestici–vol. II splancnologia. Edizione italiana a cura di Giuseppe Aureli e Bruno Ferrandi. Casa Editrice
- O’Callaghan, T. F., R. Vázquez-Fresno, A. Serra-Cayuela, E. Dong, R. Mandal, D. Hennessy, S. McAuliffe, P. Dillon, D. S. Wishart, and C. Stanton. 2018. Pasture feeding changes the bovine rumen and milk metabolome. *Metabolites* 8(2):27.
- Parker, S. P. 1988. McGraw-Hill encyclopedia of the geological sciences.
- Peng, W.-X., J. Marchal, and A. Van der Poel. 2018. Strategies to prevent and reduce mycotoxins for compound feed manufacturing. *Animal Feed Science and Technology* 237:129-153.
- Rautureau, M., C. d. S. Figueiredo Gomes, N. Liewig, and M. Katouzian-Safadi. 2017. Clay and Clay Mineral Definition. Pages 5-31 in *Clays and Health: Properties and Therapeutic Uses*. Springer International Publishing, Cham.
- Rodrigues, R., D. Ledoux, G. Rottinghaus, R. Borutova, O. Averkieva, and T. McFadden. 2019. Feed additives containing sequestrant clay minerals and inactivated yeast reduce aflatoxin excretion in milk of dairy cows. *Journal of dairy science* 102(7):6614-6623.
- Saleem, F., B. Ametaj, S. Bouatra, R. Mandal, Q. Zebeli, S. Dunn, and D. Wishart. 2012. A metabolomics approach to uncover the effects of grain diets on rumen health in dairy cows. *Journal of dairy science* 95(11):6606-6623.
- Saleem, F., S. Bouatra, A. C. Guo, N. Psychogios, R. Mandal, S. M. Dunn, B. N. Ametaj, and D. S. Wishart. 2013. The bovine ruminal fluid metabolome. *Metabolomics* 9:360-378.
- Sjaastad, Ø. V., O. Sand, K. Hove, and C. Tamanini. 2013. *Fisiologia degli animali domestici*. Casa editrice ambrosiana CEA.
- Sun, H., M. Nelson, F. Chen, and J. Husch. 2009. Soil mineral structural water loss during loss on ignition analyses. *Canadian Journal of Soil Science* 89(5):603-610.
- Sundekilde, U. K., L. B. Larsen, and H. C. Bertram. 2013. NMR-based milk metabolomics. *Metabolites* 3(2):204-222.
- Tajkarimi, M., M. A. Faghih, H. Poursoltani, A. S. Nejad, A. Motallebi, and H. Mahdavi. 2008. Lead residue levels in raw milk from different regions of Iran. *Food control* 19(5):495-498.
- Vila-Donat, P., S. Marín, V. Sanchis, and A. Ramos. 2018. A review of the mycotoxin adsorbing agents, with an emphasis on their multi-binding capacity, for animal feed decontamination. *Food and chemical toxicology* 114:246-259.
- Wang, M., H. Wang, H. Zheng, D. Uhrin, R. J. Dewhurst, and R. Roehe. 2021. Comparison of HPLC and NMR for quantification of the main volatile fatty acids in rumen digesta. *Scientific Reports* 11(1):24337.
- Winning, H., F. Larsen, R. Bro, and S. Engelsen. 2008. Quantitative analysis of NMR spectra with chemometrics. *Journal of magnetic resonance* 190(1):26-32.

- Zhang, A., H. Sun, P. Wang, Y. Han, and X. Wang. 2012. Recent and potential developments of biofluid analyses in metabolomics. *Journal of proteomics* 75(4):1079-1088.
- Zhao, S., J. Zhao, D. Bu, P. Sun, J. Wang, and Z. Dong. 2014. Metabolomics analysis reveals large effect of roughage types on rumen microbial metabolic profile in dairy cows. *Letters in applied microbiology* 59(1):79-85.